Debris Accumulation at Trash Racks Upstream of Inverted Siphons

An Exploratory Research of a Data-Driven Approach for Clogging Identification

Rijk R.P. Drenth

Delft University of Technology

TU Delft

Debris Accumulation at Trash Racks Upstream of Inverted Siphons

An Exploratory Research of a Data-Driven Approach for Clogging Identification

by

Rijk R.P. Drenth

Hydraulic and Offshore Structures
Faculty of Civil Engineering and Geosciences
Delft University of Technology

To be defended on the 11th of March 2025

Supervised by

Dr. Ir. Davide Wüthrich
Dr. Ir. Olivier A.C. Hoes

Cover: Personal photograph

TU Delft

Preface

This thesis serves as the final qualification for acquiring the degree of Master of Science in Civil Engineering and Geosciences at Delft University of Technology, for the specialization of Hydraulic and Offshore Structures. I am grateful for the lessons I have learned during the process of the research and reporting, and for the contribution and support, I would like to offer a word of thanks to the following people:

First of all, my gratitude goes out to my committee for guiding me through this process. I would like to thank Davide Wüthrich, the chair of my committee, for always being available to supervise me and provide support throughout the course of this study. My thanks also goes out to Olivier Hoes for sharing his expertise and providing me with analytical feedback.

Additionally, I am grateful for Waterschap Limburg for providing me with the data needed to realize this research. For allowing me to visit the sites and obtain valuable information. I would especially like to thank Rene Mols, Joën Corstjens, Job Heijs, Davy Nelissen and Bart van der Aa.

Finally, I would like to express my gratitude for my friends and family who morally supported me when extra motivation was needed. I could not have done this without you.

Rijk Drenth
Rotterdam, March 2025

Abstract

Accumulation of debris, and subsequent clogging of trash racks upstream of inverted siphons and culverts can pose serious inundation risks. If the upstream water level continues to rise till the banks overflow due to the blockage of the inlet, it can lead to damages and potential casualties in case of floods. Therefore, a thorough understanding of debris accumulation processes and implementation of mitigation measures in design methods is essential, even though, this is not being a common practice currently. While existing research has focused primarily on experimental studies of debris accumulations or retrospective analyses of flood events, this study leveraged datasets from Waterschap Limburg, containing water level and discharge measurements collected on site. To obtain an enhanced understanding of debris accumulation processes at trash racks upstream of inverted siphons. This research analyzed stage-discharge measurements around inverted siphons throughout Limburg to identify debris-induced anomalies in the flow conditions that corresponded to debris extractions. This process served as a foundation for a targeted investigation of these anomalies in the water levels and water level differences across the trash rack at the inverted siphon at Tungelroysebeek. Detection methods were developed to identify instances of debris removal across the dataset. This enabled an analysis of seasonal influences on the frequency of debris accumulation and extractions, where an increased occurrence of removals was found in fall months. Furthermore, Extreme Value Analysis was employed to statistically model the extreme behavior of extraction events, estimating the return periods for days with significant extractions of debris accumulations. This study demonstrated that historical water level and discharge data can be used to detect debris accumulation through stage-discharge analysis and application of identification methods. Insights were acquired on seasonal influences on the debris accumulation process, and on the likelihood of extreme accumulation events. The obtained results are expected to be useful in flood-risk assessment and development of targeted debris management strategies, and can support engineers in decision making for design and mitigation processes.

Table of Contents

Nomenclature

Abbreviations

Abbreviation	Definition
ECDF	Empirical Cumulative Distribution Function
EVA	Extreme Value Analysis
GMT	Greenwich Mean Time
GPD	Generalized Pareto Distribution
MRL	Mean Residual Life
PoT	Peak over Threshold

Symbols

Symbol	Definition	Unit
A	Cross-sectional area of the creek, upstream or downstream of the trash rack	$[m^2]$
A_{channel}	Cross-sectional area into which the siphon discharges, in this case the downstream waterway	$[m^2]$
A_{siphon}	Total cross-sectional area of the inverted siphon	$[m^2]$
B	Width of the structure and approaching waterway	$[m]$
D_{eq}	Hydraulic diameter, defined as 4 times the A_{siphon} over the P_{siphon}	$[m]$
Fr	Froude number is proportional to the ratio of flow inertia to gravitational forces ($V/\sqrt{g \cdot h}$)	$[-]$
f_{D}	Friction factor	$[-]$
g	Gravitational acceleration	$[m/s^2]$
H	Hydraulic head	$[m]$
h	Flow depth	$[m]$
h_0	Initial water depth	$[m]$
K_{friction}	Friction loss factor	$[-]$
k_{f}	Bar shape factor	$[-]$
K_{grid}	Computed grid loss factor	$[-]$
$K_{\text{grid,M}}$	Grid loss factor defined by Meusberger [2002]	$[-]$
$K_{\text{grid,R}}$	Grid loss factor defined by Ronckers [2024]	$[-]$
K_{in}	Inlet loss factor	$[-]$
K_{out}	Outlet loss factor	$[-]$
K_{tot}	Total loss factor	$[-]$
L	Length of the inverted siphon	$[m]$
P	Fluid pressure which is the hydrostatic pressure for open channel flow	$[N/m^2]$
P_{siphon}	Wetted perimeter of the inverted siphon	$[m]$
p	Blockage ratio, defined as the obstructed area over the total cross-sectional area	$[-]$
p_{debris}	Blockage ratio from debris accumulation	$[-]$
p_{grid}	Blockage ratio from the grid, corresponding to unobstructed conditions	$[-]$
Q	Discharge measured upstream	$[m^3/s]$
Re	Reynolds number, defined as the product of D_{eq} and V_{siphon} over ν	$[-]$
V	Flow velocity in the creek	$[m/s]$
V_{siphon}	Flow velocity in the inverted siphon	$[m/s]$
W_{s}	Debris solids volume	$[m^3]$
z	Ground elevation relative to NAP	[m + NAP]
ΔH	Head loss	$[m]$

Symbol	Definition	Unit
δ	Height of the structures opening, measured from the bottom of the inlet to the top of the conduit	$[m]$
ϵ	Equivalent roughness	$[m]$
ν	Viscosity of the medium	$[m^2/s]$
ρ	Density of water	$[kg/m^3]$

1 Introduction

1.1. Research context

The flooding that occurred in Belgium, Germany and the Netherlands in July 2021 following extreme and continuous rainfall, caused over 200 casualties in Belgium and Germany, as noted by Koks et al. [2022], and over 30 billion euros of infrastructural and residential damages according to Mohr et al. [2023]. Field surveys and subsequent studies demonstrated that the clogging of hydraulic structures, such as culverts and inverted siphons, caused by the accumulation of floating debris was a major factor contributing to inundation of the area. Culverts convey waterways horizontally underneath roads or dikes, and inverted siphons convey flow underneath other waterways like a canals. In an inverted siphon the water flows down first and is subsequently driven up again by the pressure due to the height difference. In the past, clogging of these culverts and inverted siphons led to significant backwater rise, subsequently resulting in elevated upstream water levels overflowing the banks, as highlighted by Ronckers [2022]. In addition to inundations, the floating debris caused structural damage to inverted siphons, culverts and other hydraulic structures along the rivers in the North-Western European catchment area, Korswagen et al. [2022].

Figure 1.1: The inverted siphon at Bunde under the Juliana Canal during high water, Abeling [2022]

Besides the extreme flooding event in 2021, culverts and inverted siphons experience clogging and consequences thereof during normal elevated flow conditions. See for instance Figure 1.1 that shows the inverted siphon at Bunde, South-Limburg under high water conditions with clear accumulation of debris on the upstream side. Existing research on flood events and the fact that during normal, elevated flow conditions, clogging due to debris accumulation can occur, highlight that an enhanced understanding of debris accumulation is essential for future flood management and the implementation in design methods.

1.2. Problem statement

The current body of research on the accumulation of debris at trash racks upstream of culverts and inverted siphons is limited, particularly with respect to continuous fieldwork observations. Most studies focused on laboratory experiments, like Schalko [2018] and Ronckers [2024], or retrospective analyses of extreme flooding events, such as Bayón et al. [2024] and Erpicum et al. [2023]. Research on identification and detection of debris accumulation under normal flow conditions has not been extensively conducted. Especially, developing detection methods through utilization of the on-site hydrological data. Furthermore, the existing knowledge on seasonal influences on debris accumulations and modeling of extreme accumulation events has not yet been explored in depth.

1.3. Research objectives

The objective of this research study is to develop methods for debris detection by utilizing datasets from on-site measuring equipment at inverted siphons throughout Limburg, in order to gain an enhanced understanding of the seasonal effects and extreme behavior of debris accumulation processes. These datasets, made available by Waterschap Limburg, contain water level and discharge measurements that will be analyzed to identify anomalies in the stage-discharge measurements that correspond to debris extractions, and therefore preceding debris accumulations. Driven by this analysis, detection methods for the identified debris-induced anomalies in the water level and water level difference across the trash rack over time will be developed. Identifying and collecting the extractions across the years facilitates a deeper understanding of the seasonal influence on accumulation and extraction occurrences. Furthermore, by statistically modeling the extreme behavior of debris accumulation, a return period can be estimated for days where significant portions of debris are expected to be removed. These research steps ought to provide in-depth knowledge and insights on debris-detection techniques, seasonal patterns and extreme occurrences of debris accumulations and extractions.

1.4. Scope

This study focuses on the effects of accumulating debris on trash racks upstream of inverted siphons that pose a natural obstacle to the floating debris flow. It includes locations where the inverted siphon's functionality could be affected by clogging and obstruction of the flow, leading to possible inundation. The considered structures are equipped with a measure for debris interception, which allows for a deeper analysis of the trash rack's role in the operations and for the development of detection methods. As well as trash racks, are the structures equipped with extraction cranes to automatically remove the accumulated debris. Moreover, this research does not distinguish between types of debris or attempts to estimate debris volumes, because the focus lies on utilizing the datasets for detection through assessment of the water level and discharge measurements. Furthermore, the associated sites are located in the Meuse catchment area in Limburg and fall under supervision of Waterschap Limburg.

1.5. Research questions

This led to forming the research questions as follows:

1. Can debris accumulations at inverted siphons be detected, utilizing on-site water level and discharge data?
2. What are the seasonal effects on debris accumulation processes, and how are they portrayed in the data?
3. How can extreme behavior in debris accumulations be demonstrated, and what is the frequency of occurrence?

1.6. Research approach

Chapter 2 includes a review of the literature where fundamentals of fluid mechanics together with established research on the characteristics of debris accumulation are highlighted. Subsequently, in Chapter 3, an overview of the obtained datasets and study locations is given. In Chapter 4 the research method is documented, where the relationship between measured water levels and discharges were utilized for the detection of anomalies. Subsequently, the identified moments in time were further analyzed in water level and water level differences across the trash rack over time to provide insights on the seasonal influences. After which, an Extreme Value Analysis is introduced for the analysis of extreme behavior and the estimation of a return period. The results of these analyses are given in Chapter 5. The established methods were employed to the datasets of other locations, to test their applicability. Chapter 6 provides a discussion of the results. Finally, in Chapter 7 concluding remarks and recommendations for further research are given.

2

Literature Review

2.1. Continuity equation and head loss in submerged culverts

Figure 2.1: Graphical representation of the continuity equation

The continuity equation is a fundamental principle in fluid mechanics, expressing the conservation of mass in a closed fluid flow system. It states that the flow rate remains constant at any point in a control volume, provided that the fluid is incompressible and the flow is steady. Figure 2.1 generally visualizes this principle. Mathematically, for two different points in the same flow system, the continuity equation is:

$$Q_{\mathrm{i}} = Q_{\mathrm{ii}} = A_{\mathrm{i}} \cdot V_{\mathrm{i}} = A_{\mathrm{ii}} \cdot V_{\mathrm{ii}} \tag{2.1}$$

In addition, the hydraulic head represents the total energy per unit weight of a fluid at a specific point in a flow system. It is a measure of the potential energy available to drive the flow, combining the effects of ground elevation, pressure, and velocity head. The hydraulic head is typically expressed by Bernoulli's equation:

$$H = \frac{P}{\rho g} + \frac{V^2}{2g} + z \tag{2.2}$$

With the hydraulic head, the continuity equation in Equation 2.1 can be applied to obtain information on the head loss over two points in the flow. The head loss represents the reduction in total head due to energy losses in a flow system, as shown in Equation 2.3. In the event of flow disruption, such as an inverted siphon in case of this research, these losses can be attributed to various factors, which will be discussed in detail in Section 2.2. For the computation of the head loss up- and downstream of the inverted siphon, the following equations can be used.

$$H_{\mathrm{i}} = H_{\mathrm{ii}} + \Delta H \tag{2.3}$$

Together with Equation 2.2, it can be rewritten by Equation 2.4. A schematic overview of the hydraulic head and the head loss over the inverted siphon is given in Figure 2.2, where the hydraulic head is depicted by the dotted line. Note that this is not a precise representation of an inverted siphon, since inverted siphons have a declining, straight and inclining section of the conduit when it conveys the flow underneath another waterway. This schematic overview attempts to clarify the hydraulic head and head loss.

$$\frac{P_{\mathrm{i}}}{\rho g} + \frac{V_{\mathrm{i}}^2}{2g} + z_{\mathrm{i}} = \frac{P_{\mathrm{ii}}}{\rho g} + \frac{V_{\mathrm{ii}}^2}{2g} + z_{\mathrm{ii}} + \Delta H \tag{2.4}$$

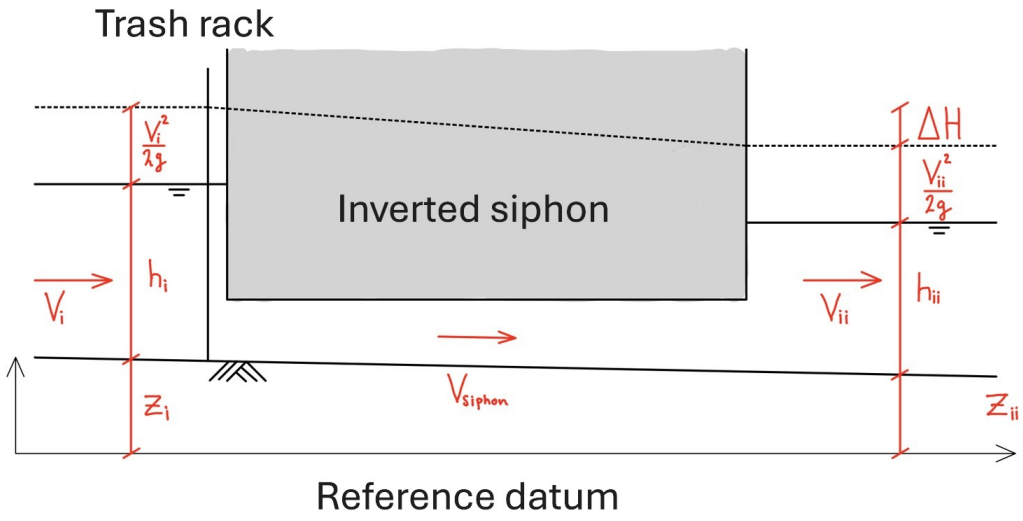

Figure 2.2: Schematic overview of the hydraulic head and head loss up- and downstream of the inverted siphon

Since at both points upstream and downstream of the inverted siphon, the pressure distribution is hydrostatic. This term is represented by the flow depth. This simplifies Equation 2.4 into Equation 2.5 which gives the following formula.

$$h_{\mathrm{i}} + \frac{V_{\mathrm{i}}^2}{2g} + z_{\mathrm{i}} = h_{\mathrm{ii}} + \frac{V_{\mathrm{ii}}^2}{2g} + z_{\mathrm{ii}} + \Delta H \tag{2.5}$$

The presence of the inverted siphon results in various energy losses in the total head. These losses are represented by the total loss factor, K_{tot}, which can be used to compute the head loss in Equation 2.6, according to Voorendt and Molenaar [2021], together with the flow velocity in the siphon.

$$\Delta H = K_{\mathrm{tot}} \cdot \frac{V_{\mathrm{siphon}}^2}{2g} \tag{2.6}$$

2.2. Loss factors

The key loss factors contributing to the total head loss over the inverted siphon are listed below.

- Inlet Losses, K_{in}: Occur when fluid enters a pipe or culvert, due to flow contraction at the entry and expansion-induced turbulence downstream of the inlet.
- Outlet Losses, K_{out}: Occur as fluid exits a system, influenced by the cross-sectional areas of the conduit and receiving waterway.
- Frictional Losses, K_{friction}: Energy is lost due to friction between the fluid and pipe's inner surface.
- Grid Losses, K_{grid}: Arise when flow passes through trash racks, causing a head drop based on trash rack lay-out and flow conditions.

It is important to note that in addition of this list, other loss factors may influence the head loss, such as losses due to bends or junctions. However, if junctions are absent and the bends do not exceed 15 degrees, they can be ignored, according to Schall et al. [2012]. The total loss factor is therefore given by Equation 2.7, and the following sections contain elaborations on the considered loss factors. Note that the loss factors listed above are not constant but their influence becomes greater with higher flow velocities.

$$K_{\text{tot}} = K_{\text{in}} + K_{\text{out}} + K_{\text{f}} + K_{\text{grid}} \tag{2.7}$$

2.2.1. Inlet loss factor

The inlet loss factor is dependent on the type of inlet and material of the conduit. For a headwall perpendicular to the embankment without any wingwalls present, Schall et al. [2012] state that the inlet loss factor is about 0.5 for a squared-edged, concrete inlet of circular conduits.

$$K_{\text{in}} = 0.5 \tag{2.8}$$

2.2.2. Outlet loss factor

Tullis [2012] proposes Equation 2.9 for the outlet loss factor which is based on the ratio of the cross-sectional area of the inverted siphon (A_{siphon}) to the cross-sectional area of the channel into which it discharges (A_{channel}). This relationship accounts for the Borda-Carnot expansion loss, which occurs due to the sudden expansion of flow from the inverted siphon into the wider channel.

$$K_{\text{out}} = \left(1 - \left(\frac{A_{\text{siphon}}}{A_{\text{channel}}}\right)\right)^2 \tag{2.9}$$

2.2.3. Friction loss factor

Friction loss factor is defined by the Darcy-Weisbach formula in Equation 2.10 for pressurised pipe-flow, with L representing the length of the inverted siphon.

$$K_{\text{friction}} = f_{\text{D}} \cdot \frac{L}{D_{\text{eq}}} \tag{2.10}$$

Here, D_{eq} is the hydraulic diameter which is defined below in Equation 2.11, where A is the cross-sectional area of the flow, and P is the wetted perimeter (the portion of the perimeter in contact with the fluid). Since, in this study, all inverted siphons are submerged, A_{siphon} is the cross-sectional area of the inverted siphon, and P its perimeter.

$$D_{\text{eq}} = \frac{4A_{\text{siphon}}}{P_{\text{siphon}}} \tag{2.11}$$

The friction factor, f_{D}, can be iteratively found in the Colebrook-White formula in Equation 2.12 for turbulent flow (Re > 4000). Here, ϵ represents the equivalent roughness which is assumed to be 0.0003 meter for concrete, Shashi Menon [2015].

$$\frac{1}{\sqrt{f_{\text{D}}}} = 1.14 - 2\log_{10}\left(\frac{\epsilon}{D_{\text{eq}}} + \frac{9.35}{Re\sqrt{f_{\text{D}}}}\right) \tag{2.12}$$

The Reynolds number is defined in Equation 2.13, where V_{siphon} is the flow velocity in the inverted siphon and the ν is the kinematic viscosity of the medium, which is 1.0e-6 m^2/s for water at approximately 20 °C.

$$Re = \frac{D_{\text{eq}} \cdot V_{\text{siphon}}}{\nu} \tag{2.13}$$

2.2.4. Grid loss factor

Meusberger [2002] proposes Equation 2.14 for the computation of the grid loss factor, which contains the blockage ratio, p, which is the ratio of the total area comprising the obstruction, the trash rack in this case, to the cross-sectional area of the channel, and the bar shape factor, k_f after Kirschmer [1928].

$$K_{grid,M} = k_f \cdot \left(\frac{p}{1-p}\right)^{\frac{3}{2}} \tag{2.14}$$

Moreover, Ronckers [2024] proposed an engineering application that computes the expected head loss as backwater rise. This computation employs an updated equation for the $K_{grid,R}$ in Equation 2.15 that only depends on the blockage ratio, which makes the formula also suitable for more general obstructions like debris accumulations.

$$K_{grid,R} = (1 + 1.37p + 0.78p^2) \cdot \frac{p}{1-p} \tag{2.15}$$

It also includes the calculation of the combined blockage ratio due to the trash rack, p_{grid}, and present debris, p_{debris}. It is depicted in Equation 2.16.

$$p = p_{grid} + p_{debris} \cdot (1 - p_{grid}) \tag{2.16}$$

Furthermore, it enables the computation of total expected debris volume based of the Equation 2.17, which incorporates dimensions like the width of the structure, B, height of the opening, δ, and upstream water depth, h_0. Here, it is crucial that the structure is fully submerged and has an outflow control regime.

$$p_{debris} = 0.17 \cdot \ln(1 + 2.78 \cdot \frac{V_s}{B \cdot \delta^2}) \cdot (\frac{h_0}{\delta})^{-0.45} \tag{2.17}$$

2.3. Head loss over trash rack

In this research, the focus is only on the head loss over the trash rack, since it was proven to be useful for the detection of debris accumulation. Therefore, the configuration shifts to considering solely the hydraulic head up- and downstream of the trash rack, as can be seen in Figure 2.3. As a result, loss factors that account for the inlet, outlet and frictions losses do not apply any longer. They were included to provide insights on the loss processes. Now, only obstruction of the flow by the trash rack and accumulated debris, contributes to the head loss. The computation of the head loss by means of the continuity equation in Equation 2.5 changes into Equation 2.18, because it can be assumed that the ground elevation upstream and downstream of the trash rack is the same.

$$h_i + \frac{V_i^2}{2g} = h_{ii} + \frac{V_{ii}^2}{2g} + \Delta H \tag{2.18}$$

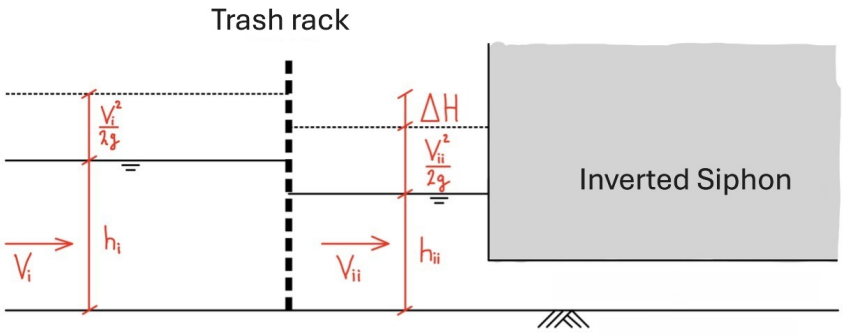

Figure 2.3: Schematic overview of the hydraulic head and head loss up- and downstream of the trash rack

2.4. Experimental insights on accumulation characteristics

Bocchiola et al. [2008] and Schmocker and Hager [2011] demonstrated in their research on wooden debris blockage at piers or columns that the probability of large woody debris becoming trapped, either at a single pier or between two piers, decreases as the Froude number increases. The Froude number, proportional to the ratio of flow inertia to gravitational forces, is provided in Equation 2.19. Lower Froude numbers result in greater relative width and length of debris accumulations, while higher Froude numbers increase relative depth, according to Panici and De Almeida [2018]. In addition, higher Froude numbers and lower initial water depths lead to an increased relative backwater rise, shown by Erpicum et al. [2023] and Burghardt et al. [2024].

$$Fr \propto \frac{\text{inertia}}{\text{gravitation}} = \frac{V}{\sqrt{g \cdot h}} \tag{2.19}$$

Schmocker and Hager [2011] revealed that blocking probability also rises with decreasing freeboard and larger drift dimensions. When pier or column spacing closely matches log length, entrapment becomes more likely, proven by Bocchiola et al. [2008]. Higher log lengths and more piers increase accumulation, while a wider span, hence fewer piers, reduces clogging, according to Schalko [2018] and Erpicum et al. [2023]. Furthermore, Schalko [2018] showed that higher Froude numbers and accumulation length, along with lower debris compactness and log diameters, further raise backwater levels. However, in cases where the wood accumulation can freely develop at a single pier, see Figure 2.4 later-arriving debris has a lesser impact on backwater rise. Ronckers et al. [2024] also highlight the dependence of accumulation geometry on hydraulic conditions for submerged culverts, where higher Froude numbers tend to result in more compact accumulations where debris is pulled down towards the bottom.

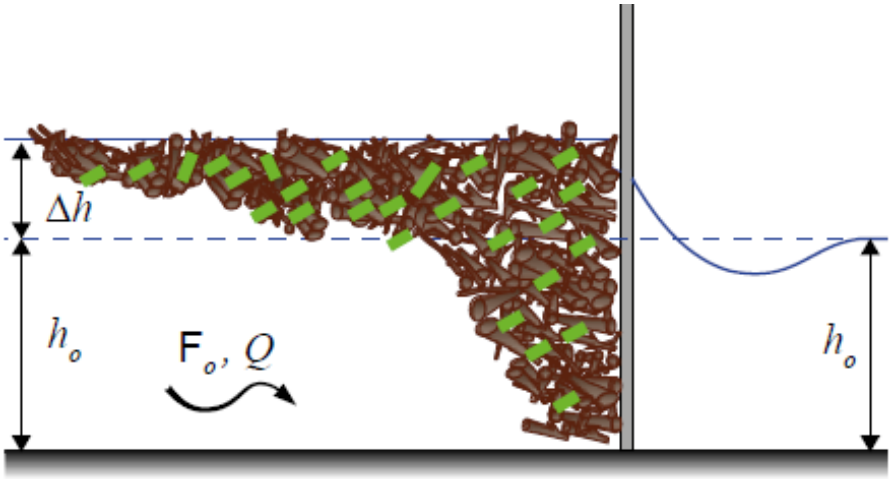

Figure 2.4: Experiment set-up for accumulation of wood. Schalko [2018]

2.5. Effects of debris composition

Debris in waterways includes both organic and human-made materials, each influencing hydrodynamic conditions differently. Through experimental tests Schalko [2018] showed that fine organic debris, such as branches and leaves, tends to reduce permeability and increase flow diversion, leading to a higher backwater rise. Similarly, debris accumulation at the inverted siphon at Bunde, Limburg was analyzed by Ronckers [2022], who classified debris based on length, diameter, and length-to-diameter ratio. Following the 2021 floods, large branches caused a 4.1% blockage, while bundles with leaves contributed to a 9.6% blockage, accounting for porosity. Subsequent observations in 2022 noted smaller debris pieces, leading to capacity reductions of up to 8.3%. However, not all debris consists of natural material. Plastic and other human-made materials, due to their low porosity and high flexibility, also contribute significantly to debris accumulation. Via flume experiments Honingh et al. [2020] found that plastics in debris compositions led to faster, denser blockages.

Furthermore, post-flood field research in Germany's Ahr Valley by Korswagen et al. [2022] also identified trees, branches, and local vegetation as primary contributors to debris accumulation. This organic debris, through its interlocking nature, formed blockages on the upstream side of structures during the 2021 floods. In addition, in the EM Flood Resilience Project debris accumulation after the extreme 2021 flood event was examined. Data from clogged bridges and culverts in the Meuse and Rhine catchment areas showed that around 50% of the debris consisted of human-made materials, as can be seen in Figure 2.5. Analysis from Erpicum et al. [2023] revealed that most debris accumulates at structures with small span widths, thus making culverts and inverted siphons specifically vulnerable. Laboratory tests from this project further demonstrated that mixing debris types can amplify hydrodynamic impacts. For instance, a 50/50 composition of logs and flat objects like building rubble increased backwater rise by 150% compared to logs alone, Erpicum et al. [2023] and Burghardt et al. [2024].

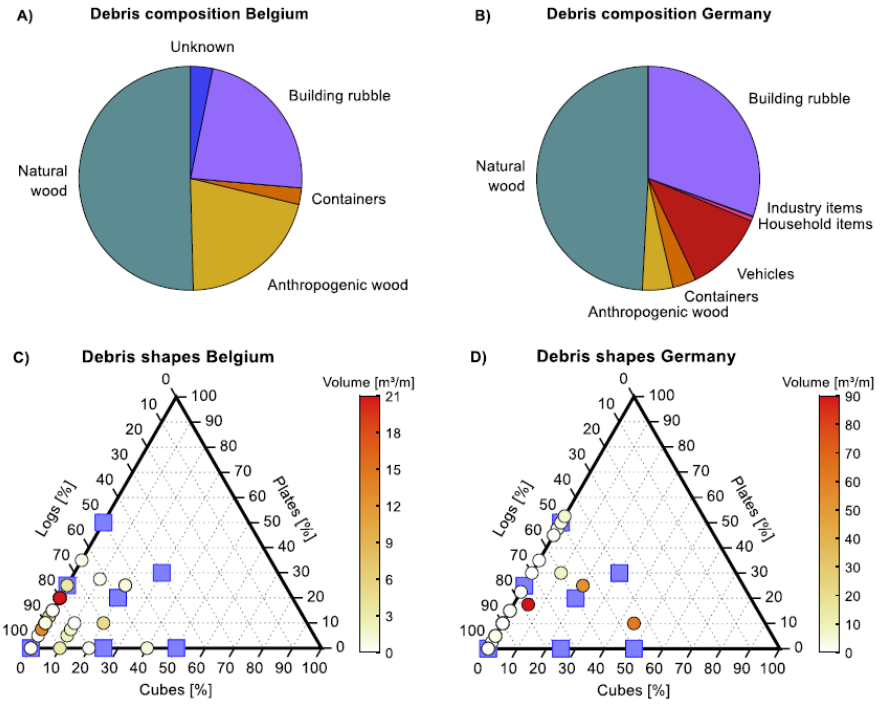

Figure 2.5: Debris compositions observed form the field data after the 2021 flood event. Erpicum et al. [2023]

2.6. Field work observations

Thus far, the research based on field work observations was conducted to obtain information on debris compositions, accumulation development and structural damage in the area after floods. These field work analyses rely on different observation techniques. For example, Lyn et al. [2007] periodically visited bridge piers in Indiana to categorize debris accumulations at different sites, while, Korswagen et al. [2022] evaluated damages induced by the 2021 July flood in the Ahr valley, by means of an extensive field survey. Similarly, Bayón et al. [2024] analyzed debris accumulations from major floods worldwide in order to categorize debris composition, frequency and prevalence. Similarly, Erpicum et al. [2023] created a database focusing on structural properties, hydraulic conditions, and debris accumulation characteristics. These researches relied on the use of photographs made during site visits or by bystanders on site, and showed the dependence of images in the analysis of debris.

Whereas, Lyn et al. [2003] used video imagery for the capturing of movements and accumulations of debris at bridge piers during high-flow events in Indiana. In extension to this research, debris transport was continuously monitored through video cameras at three sites in Indiana, Lyn et al. [2007]. For both researches, the obtained information on debris accumulation properties, was coupled with hydrological data from nearby gauging stations. It was found that debris transport was noticeably heavier during the early rising part of the flow event. Additionally, Wyss et al. [2021] used video recordings to qualitatively assess the accumulation of large wooden debris at a bridge pier on the Glatt River, Zurich, correlating field observations with laboratory findings by Schalko et al. [2019] to demonstrate the scalability of experimental results to real-world scenarios. Lastly, Kataoka and Nihei [2020] developed a new technology to quantify macro-debris in riverine environments, which gathers images from video monitoring, validated through both lab experiments and field tests at the Node Bridge over the Edo River.

Moreover, Honingh et al. [2020] conducted a research through field measurements in the Cikapundung River in Indonesia, where samples were taken from the river to examine the compositions of the debris and the varied effects different materials have on accumulation behavior. It was also highlighted that at the start of intense rainfall, the water level rises and floating debris is collected. The combination of increased flow velocity and plastic debris transport made accumulations at the trawl more likely.

2.7. Rating curves

Rating curves are essential tools in hydrology. They provide a relationship between the stage (water level) and the discharge (flow rate) of a river or stream, shown by Rantz [1982]. Typically constructed using empirical methods, these rating curves are generated from extensive data collection at gauging stations. Once established, rating curves enable us to estimate flow rates in areas where direct monitoring measurement of discharge and flow velocity is complicated. However, discharge measurement is a complex process, with flow velocity measurement being particularly labor-intensive. Typically, rating curves are derived using a one-to-one method, where discharge is measured under quasi-steady flow conditions, thus limiting the applicability during unsteady, extreme conditions such as floods Muste et al. [2010]. Notably, maximum water levels and maximum discharge do not always coincide at a single location; rising parts of the flood wave often exhibit higher flow velocities than trailing flows Muste et al. [2010]. This velocity variation presents itself as a double-sided loop, or hysteresis effect, in rating curves, as shown in Figure 2.6.

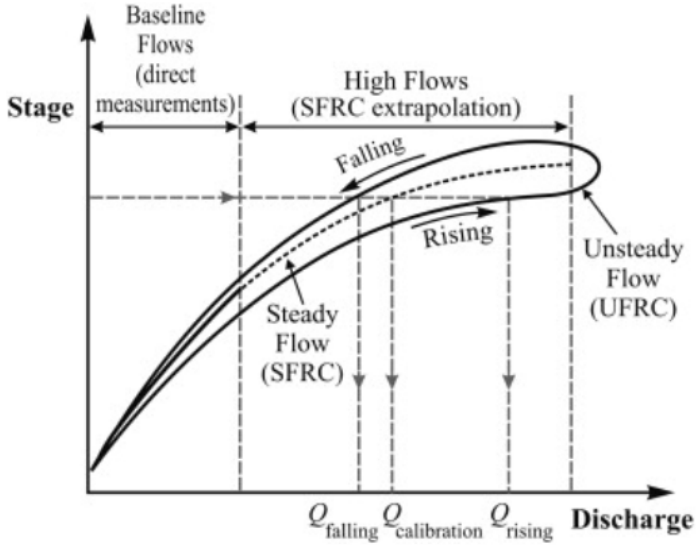

Figure 2.6: Double-sided loop in rating curve during flood event, Muste et al. [2010]

For a rating curve to be a reliable tool, the use of accurate and high-quality measurements obtained from well-calibrated equipment is crucial. Flow velocity and stage measurements, as well as flow depth and distance across the channel between observation verticals, are used to construct a relationship between the water level and the discharge according to Herschy [2009]. It is essential that the flow velocity and the water level are measured at the same location to generate rating curves. If so, they can be used in case of situations where direct measuring is challenging and deployment of rating curves is necessary. In the case of this research, this condition can not be guaranteed, as the discharge and water level data are being measured at different gauges, and no direct relationship can be assumed between the two. Therefore, discharge-water level measurements, Q-h measurements, will be referred to for the detection of anomalies in the flow regime. They are introduced in Section 3.1. The Q-h measurements carry higher uncertainty, but still offer valuable insights.

2.8. Knowledge gap

Despite extensive laboratory research on debris blocking probabilities and backwater rise influenced by parameters such as Froude numbers, debris composition, and structural dimensions, there is limited knowledge on how the utilization of on-site water level and discharge measurements can support in effectively detecting present debris, even though it is common for culverts and inverted siphons to be monitored permanently. Existing fieldwork has relied on observational data, such as camera images, which, while insightful, were not linked to measurements of the flow conditions. The integration of measured head loss, as a tool for debris detection, has not been explored. Also the examination of Q-h measurements and temporal water level variations to discover debris-induced anomalies in the flow conditions, have not been thoroughly investigated. Furthermore, seasonal effects and extreme debris accumulation behavior remain underexplored. This research addresses these limitations by leveraging historical data of on-site measurements to couple observed anomalies in Q-h measurements, water level plots, and head loss computations, to the presence of debris accumulations.

3

Study Locations

Four research locations situated in smaller creeks within the Meuse basin in Limburg were selected for this analysis. The first site is an inverted siphons equipped with a trash rack located in the Tungelroysebeek, and the second, an inverted siphon in the Geul at Bunde. The other sites, an inverted siphon with a trash rack in the Uffelsebeek and a trash rack in the Groote Molenbeek at Wanssum, were obtained in a later research phase. At Bunde a trash rack is not present, and despite the objective focusing on debris accumulations at trash racks upstream of inverted siphons, it was still useful to investigate this site. Figure 3.1 shows in the map of Limburg where these sites are located.

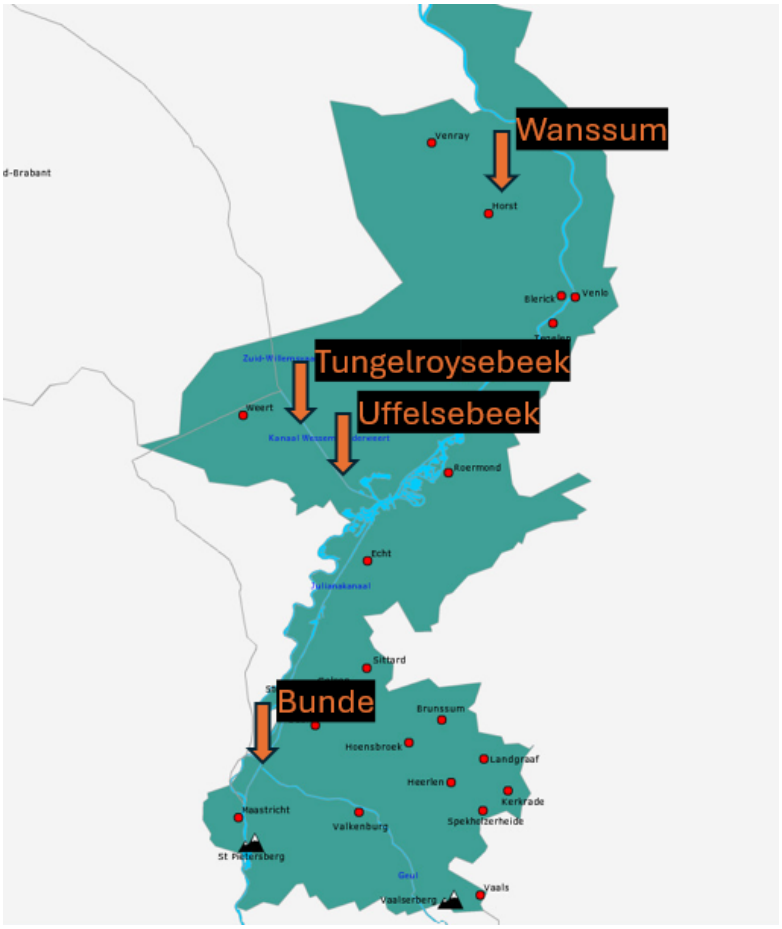

Figure 3.1: Research locations on the map of Limburg

3.1. Overview of the datasets

The datasets, provided by Waterschap Limburg, contain years of historical data on water levels, with different purposes. Some water level measurements are used for triggering extraction sequences, where others are used for discharge computation, and others serve purely as a water elevation indicator. All water level sensors measure in GMT+1. Table 3.1 gives an overview of the available information.

	Water level	Timeframe	Instrument type	Error margin	Interval times
Tungelroysebeek	Upstream of trash rack	2004 - 2024	Pressure sensor	± 2 cm	15 min
	Downstream of trash rack	2004 - 2024	Radar sensor	± 2 cm	15 min
Bunde	Upstream of inverted siphon	2015 - 2024	-	-	15 min
	Downstream of inverted siphon	2022 - 2024	-	-	15 min
Uffelsebeek	Upstream of trash rack	2004 - 2024	Pressure sensor	± 2 cm	15 min
	Downstream of trash rack	2004 - 2024	Radar sensor	± 2 cm	15 min
Wanssum	Upstream of trash rack	2020 - 2024	Pressure sensor	± 2 cm	15 min
	Downstream of trash rack	2020 - 2024	Radar sensor	± 2 cm	15 min

Table 3.1: Overview of the measured water levels across the sites

The discharge is calculated based on the cross-sectional area, from measurements of the water level and flow velocity. The flow velocities are measured at a fixed height. The flow velocities are then divided in different cells of the cross-sectional area, after which the mean flow velocities are derived. Finally, by means of design formulae, the discharge is computed and therefore not measured independently. For Tungelroysebeek and Bunde the discharge is determined in close proximity of the site. For Uffelsebeek and Wanssum, the discharge is derived from available measurement gauges further upstream of structure. Furthermore, it is important to note that the datasets contain significant gaps in the data within single years or over several years, because of technical defects, or natural reasons like the water level at high water exceeding the measuring instrument's height. For instance, the discharge dataset at Tungelroysebeek has almost continuous measurements from 2021 till 2024, and intermittently, discharge was recorded in 2010 and 2011. All discharge data is measured in GMT+1. Table 3.2 provides an overview of the discharge data as provided by the waterboard. Here, the last column shows whether additional inflow of water can be excluded in between the instrument and the structure.

	Timeframe	Interval times	Distance to the structure	Additional inflow excluded?
Tungelroysebeek	2010 - 2024	15 min	~ 300 m	Yes
Bunde	2004 - 2024	15 min	~ 925 m	Yes
Uffelsebeek	2004 - 2024	15 min	~ 4.6 km	No
Wanssum	2020 - 2024	15 min	~ 1 km	No

Table 3.2: Overview of the measured discharge across the sites

3.2. Hydraulic characteristics of the selected locations

All sites are located in the Meuse catchment basin, but in smaller creeks and rivers that are tributaries of the Meuse. Table 3.3 gives an overview of the rivers and their characteristics. The mean values are derived from the sources listed below or, when online data are unavailable, are estimated based on values from the provided datasets. It is important to realize that for extreme conditions, the measurement equipment is not reliable since gauges get destroyed or are too small dimensioned, according to Roggenkamp and Herget [2024]. That is why often the maximum discharge values here are estimated by means of hydraulic models and statistical analysis originating from the 2021 floods, where the process of precipitation transition into discharge is modeled, shown by De Jong and Asselman [2022] and van Heeringen et al. [2022].

	Meuse (at Maastricht)	Tungelroysebeek	Geul
Length $[km]$	940	26	58
Mean flow rate $[m^3/s]$	250	2	4
Max flow rate $[m^3/s]$	3310	-	110
Basin area $[km^2]$	36000	157	340
	Uffelsebeek	Groote Molenbeek	
Length $[km]$	44	32	
Mean flow rate $[m^3/s]$	1	3	
Max flow rate $[m^3/s]$	-	-	
Basin area $[km^2]$	223	180	

Table 3.3: Overview river information; waterschap Overmaas en Roer [2016], zuiveringschap Limburg [2002], Rijkswaterstaat [2024], Rijkswaterstaat [2021], PDOK [2024]

3.3. Tungelroysebeek

The first site is located in the Tungelroysebeek, and consists of an inverted siphon with a debris rack and extraction crane, that conveys the creek under the Wessem-Nederweert Canal, see the overview in Figure 3.2. Site details are included in Appendix A.1. At this site, multiple measuring instruments are present, but they vary in accuracy and measuring intervals. Instruments upstream and downstream of the trash rack require lower precision and are not adequately calibrated. They serve primarily as alerts to trigger extraction when the stage difference across the trash rack exceeds 35 cm, which occurs seldom according to the local operator. Measurement errors can lead up to 2 cm difference per sensor, so, 4 cm in the worst case. Furthermore, the deployment of the extraction crane is periodically scheduled at 11:30 and 23:30, and according to the inspector of this site, this is sufficient for adequate operation throughout the year. However, inspectors of the structure can manually initiate a cleaning sequence if they deem it necessary, and this occurs occasionally in autumn months with leaf fall being more frequent. So, under normal conditions, debris is removed automatically through one of the aforementioned methods in a cleaning sequence lasting approximately 10 minutes. However, in times of extreme discharge, tractors are deployed to pump excess water into the canal, and the inspector must manually navigate the crane. The inspector also noted that the crane is sensitive in case of increased weight during snowfall or frost, as even a slight sway along the trajectory can result in malfunction.

Figure 3.2: Overview of the inverted siphon with trash rack and extraction crane at Tungelroysebeek

The discharge observed in the dataset has a mean value of 1.21 m^3/s and a maximum of 7.02 m^3/s. Note again that maximum discharges are often underestimated, since the instruments can overflow or get destroyed. Similarly, the recorded water level measurements provide a reasonable insight. However, extreme values for water levels tend to be higher in reality. Mean water levels upstream of the structure are observed at 25.52 m + NAP and downstream at 25.47 m + NAP.

3.4. Bunde

The inverted siphon at Bunde conveys the Geul underneath the Juliana Canal where it flows into the Meuse, see Appendix A.2. The siphon consists of five rectangular conduits, with gates that can be closed or opened depending on the flow conditions. It is an interesting site because, in response to the flooding event of July 2021, four columns were placed in front of the structure to intercept branches and reduce the accumulation of debris, see Figure 3.3 for an overview. Unlike in the Tungelroysebeek, there is no debris rack, nor extraction crane present, so, the debris removal, when reaching a critical state, occurs manually. The site was included since it was a relevant site in previous research on debris accumulations at inverted siphons by Ronckers [2022], and it played an important role in the exploratory phase of this study. The discharge at the Geul is measured further upstream of the structure. However, since no additional inflow occurs between the measurement point and the siphon, the data are still deemed reliable for analysis.

Figure 3.3: Overview of the inverted siphon and interception columns on the upstream side at Bunde

Moreover, a mean discharge of 3.25 m^3/s was observed from the extensive dataset. Note again that peak discharges during extreme flood conditions are not recorded, so, through hydraulic models that transition precipitation into discharge, the actual peak discharge values for the July 2021 flood were estimated to range from 85 - 110 m^3/s by De Jong and Asselman [2022]. Furthermore, water levels under normal conditions are measured around 41.4 m + NAP upstream and 41.2 m + NAP downstream. As for the discharge, measured water levels during extreme conditions are not representative. The peak water levels are estimated to be at least 4 meters higher than average values during the 2021 flood, which had an exceedance probability between 1:100 and 1:1000 per year, shown by De Jong and Asselman [2022].

3.5. Uffelsebeek

The third location is the inverted siphon in the Uffelsebeek which conveys the creek underneath the same Wessem-Nederweert Canal as the Tungelroysebeek, see Figure 3.4. Similar to the Tungelroysebeek, the upstream and downstream water levels of the trash rack are measured using the same type of instruments. Additionally, the extraction method—twice daily, triggered by exceedance, or upon inspection—is identical. The discharge is measured close the border with Belgium, which is 4.6 km upstream. This distance and the fact that additional water inflow cannot be excluded, makes the dataset less reliable for use. See Appendix A.3 for a site overview.

Figure 3.4: Overview of the inverted siphon with trash rack and extraction crane at Uffelsebeek

3.6. Wanssum

The fourth location is a single trash rack at Wanssum situated in the Groote Molenbeek, see Figure 3.5. This structure, as opposed to the other locations, is not near an inverted siphon, but it is a single trash rack with extraction crane that enables the removal of debris before the creek expands its width. The discharge is measured approximately 1 km upstream of the structure, with additional inflow from other waterways contributing downstream. Furthermore, Waterschap Limburg noted that during periods of significantly high water levels and simultaneous clogging of the trash rack, flow alongside the structure can occur, bypassing the trash rack. These factors raise concerns about the dataset's reliability, as the measured extreme water levels and overall discharge values are likely underestimated.

Figure 3.5: Overview of the trash rack at Wanssum

4

Research Methods

Section 4.1 introduces the method to detect debris-induced anomalies in the Q-h measurements. Section 4.2 provides the method for further investigation of the water variations, driven by the identified anomalies, and shows the methods and conditions used for detection of debris accumulations throughout the whole dataset. Section 4.3 introduces the methodology of the applied EVA. Section 4.4 tests the established methods by applying them to other datasets. The results of the analyses are found in Chapter 5.

4.1. Anomaly detection in the Q-h measurements

In this research phase, Q-h measurements were evaluated to analyze the flow conditions at Tungelroysebeek and Bunde, and therefore aimed to identify and explore debris-induced anomalies in the flow conditions. These Q-h measurements were color-coded to highlight monthly variations within each year and occasionally refined to monthly and daily intervals. By examining the Q-h measurements, normal, unobstructed conditions were identified and subsequently, anomalies in the flow regime that may suggest accumulations or the removal of debris. Subsequently, the promising anomalies were further explored by looking into water level behavior over time as well as the difference in water level up- and downstream of the trash rack. Several cases that display irregularities were investigated, however, only one type of anomaly was deemed useful for further research. The promising type of anomaly was found after the examination of the Q-h measurements of 2010 and 2011 of Tungelroysebeek, where a recurring phenomenon was observed; the water level continued to rise and drop for a, more or less, constant discharge, forming "columns". Figure 4.1 displays a schematic representation of the observed event. In other cases, where the analysis showed less insightful results, the abnormal behavior was sometimes observed over the course of days or months even, where debris accumulation can occur over the course of hours. Furthermore, the fact that it was challenging to determine whether the observed anomalies were actually induced by debris presence, proved that these anomalies were not promising enough to further investigate. The analyses for these cases are included in Appendix B.

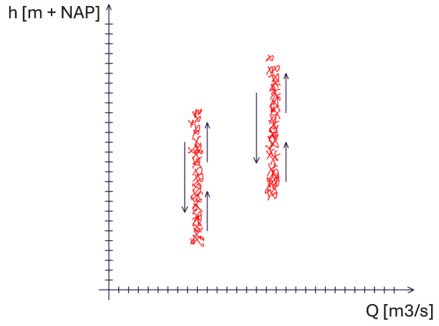

Figure 4.1: Graphical representation of sharp drops in Q-h measurements

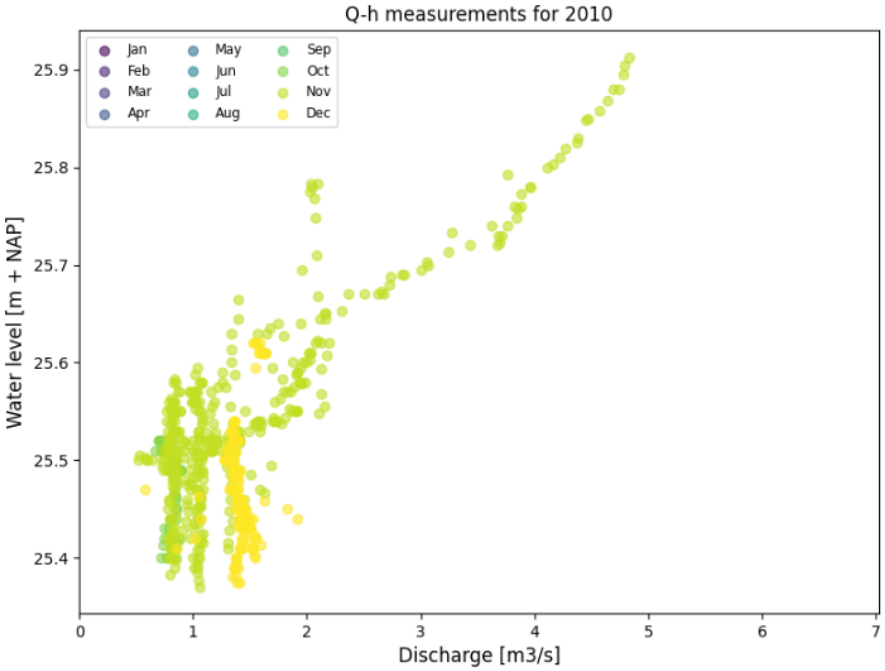

Figure 4.2: Q-h measurements at Tungelroysebeek in 2010

Figure 4.2 shows the Q-h measurements of all available data from 2010 at Tungelroysebeek, where the data from November are represented by the light green markers. Here it becomes evident from the course of the water level in the Q-h measurements for November, that for a portion of the data, the water level fluctuates approximately 20 cm, while the discharge remains relatively constant. Similarly, the December data, which is represented by the yellow markers, comparable fluctuations were observed. Both months' individual Q-h measurements are displayed for a range of days in Figures 4.3 and 4.4, where this observation is evident.

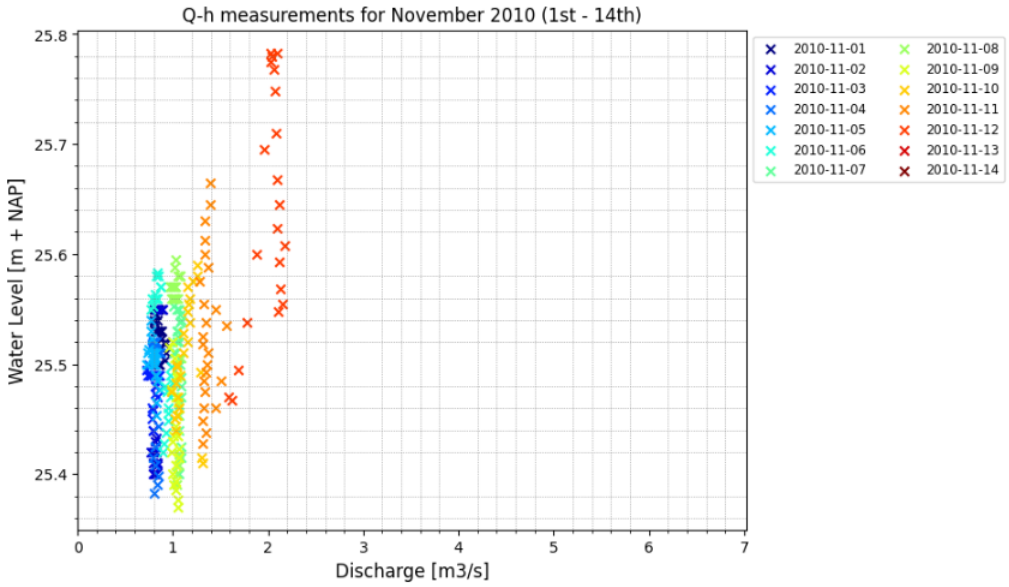

Figure 4.3: "Columns" in Q-h measurements at Tungelroysebeek in November 2010 (1st - 14th)

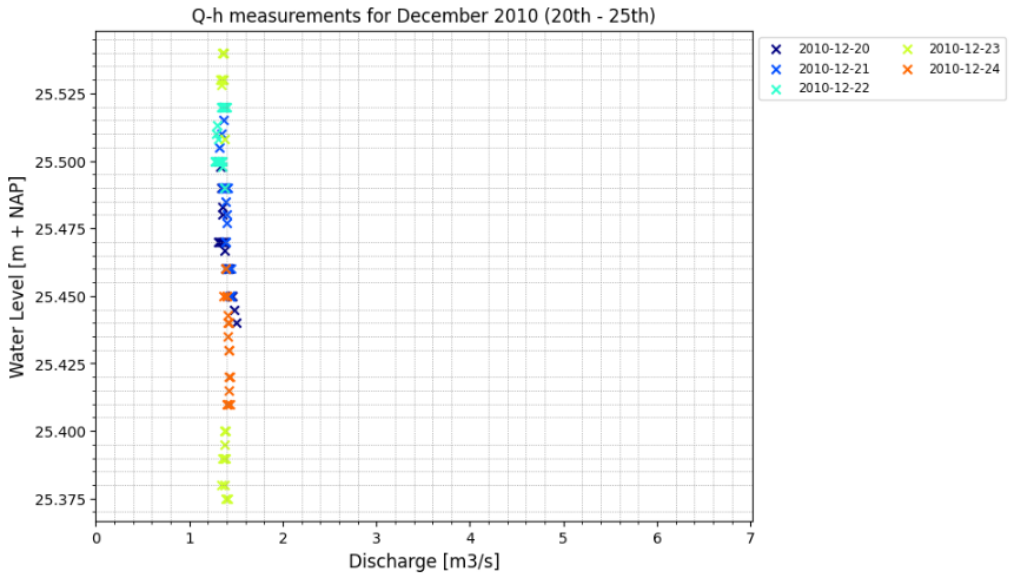

Figure 4.4: "Columns" in Q-h measurements at Tungelroysebeek in December 2010 (20th -25th)

The formation of these "columns" suggests the initial stages of debris accumulation which acts as blockage, causing the water level to rise progressively. The subsequent drops in water levels, for a constant discharge, could be the result of the extraction of debris. To investigate this hypothesis further, the water level over time for the first two weeks of November is analyzed, as shown in Figure 4.5. In this plot the significant, sharp drops are clearly visible, and therefore show potential for further analysis.

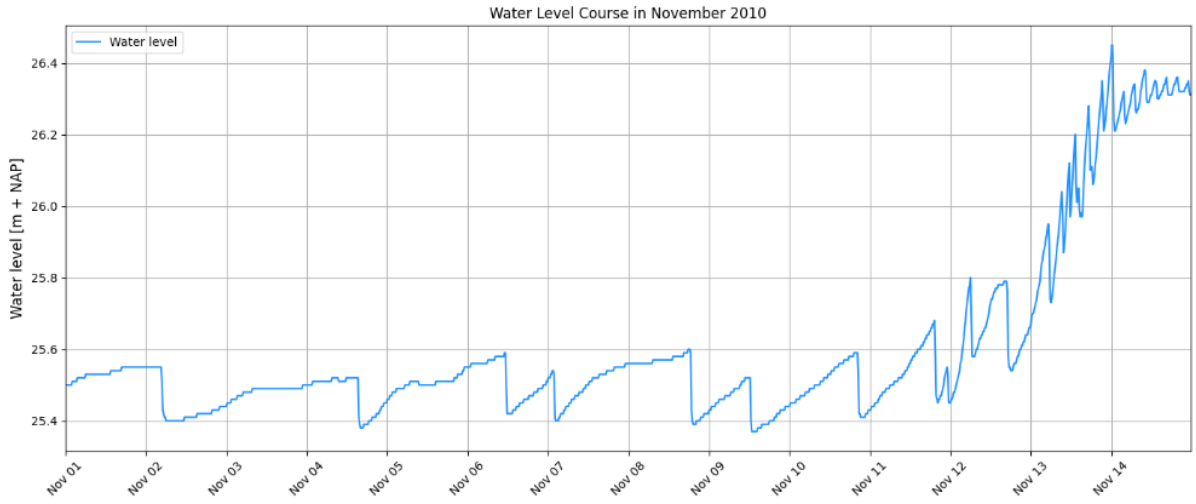

Figure 4.5: Water level at Tungelroysebeek in November 2010

The observed extractions that were identified in the Q-h measurement analysis, seem to occur, after visual judgment, between October and March. This seasonality suggests that the fall and winter months, characterized by higher flow conditions and more fallen leafs and branches, are particularly susceptible to these events. In Sections 4.2.1 and 4.2.2, the focus was laid on exploring and further analyzing the sharp drops in the water level variations. This allows for the investigation of the seasonal influence on the frequency of occurrence. Note, that during this phase of the research, Q-h measurements were created and analyzed for both Tungelroysebeek and Bunde. However, in the coming stages, only the data from Tungelroysebeek (later on also Uffelsebeek and Wanssum) were used due to the absence of a trash rack and extraction crane at Bunde, as the sharp drops potentially indicate trash removals.

4.2. Investigation of the water level variations

4.2.1. Water level over time

It was found in the analysis in Section 4.1 that the occurrence of "columns", corresponded to sharp drops in the water level. To better understand the frequency of occurrence and seasonality of the observed sharp drops, detection methods were developed for the Tungelroysebeek dataset using signaling plots in the water level over time. These plots highlight the sharp drops, or detected debris extractions, within the annual water level data over time, see for instance Figure 4.6 for the water level plotted for 2017 at Tungelroysebeek together with the markings of the occurrences.

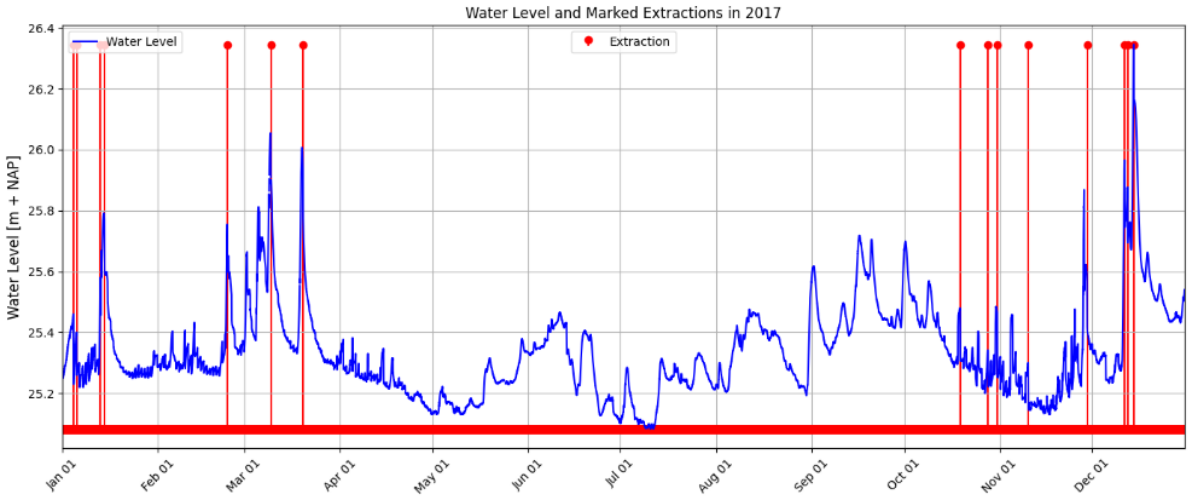

Figure 4.6: Water level and marked extractions at Tungelroysebeek in 2017

The markings in these plots are triggered based on specific conditions designed to indicate sharp drops in the water level suggesting removal of debris. These conditions are listed below:

A1. A sharp drop was marked when the water level decreased by 10 cm or more within two consecutive measurement points, corresponding to a 30 minute interval, providing a margin to ensure comprehensive detection.

A2. To ensure the water level increases gradually towards a sharp drop, this condition imposed a threshold on the rise of the water level preceding the drop. Cases where two consecutive measurement points rise more than 10 cm within 24 hours before the drop, were excluded. Therefore, sharp drops caused by an abrupt rise of discharge or water level were left out, ensuring that these are reliably associated with possible debris accumulations and extractions

A3. Immediately after detecting a sharp drop, the water level difference up- and downstream of the trash rack must fall within -2 cm to 2 cm, reflecting the precision of the instruments. This ensures that the event represents debris extraction, as the trash rack should be unobstructed after the sharp drop in water level.

An estimation was made for the selection of these conditions upon examination of the water level plots. However, to better argue the selection, a sensitivity analysis was performed on the conditions. This analysis provides an outlook on the influence an input parameter value has on the results by validating parameter-combinations for a range of values. Condition A1. showed to be sensitive to lower threshold values where a significant number of removal events would be detected. In contrast, selecting higher parameter values would reduce the number of detected events greatly. Therefore, careful calibration of this condition included ensuring the capture of significant sharp drops while excluding minor deviations. Condition A2. showed that higher thresholds did not lead to more detected drops, thus proving less sensitive to changes, only reducing the threshold value would also reduce the number of detected removal events. Condition A3. exhibited some sensitivity to higher threshold values, however, reflects the accuracy of the instruments rather than a hand-selected condition. Visual representations of the sensitivity analysis can be found in Appendix C.1.

4.2.2. Water level difference across the trash rack over time

In addition to first the detection method that focused on analyzing the upstream water level of the trash rack over time, a second detection method was developed for a more comprehensive representation. This method analyzed the water level difference up- and downstream of the trash rack over time, to better encompass the behavior of the water level across the trash rack driven by potential debris presence and the removal thereof. This method also utilized signaling plots to pinpoint extraction moments by means of markings, with a set of conditions as follows:

B1. Debris presence is hypothesized if the water level difference across the trash rack surpasses the mean head loss value across the trash rack. This value is computed with Equation 2.18 where the flow velocity up- and downstream of the trash rack are computed with the overall, mean discharge. This mean head loss is approximately 5 cm, plus a 10 cm margin, resulting in a (conservatory) exceedance threshold of 15 cm.

B2. Under normal conditions flow obstruction is not expected, represented by head losses below the mean value of 5 cm. So, if the water level difference up- and downstream returns below this baseline within 30 minutes after an exceedance, it suggests debris has been removed crane.

Even though the Condition B1. and B2. are physically supported, since they represent potentially clogged and unclogged conditions, a sensitivity analysis was conducted, whose the results are in Appendix C.1. Here it was found that Condition B1. showed sensitivity to changing threshold values, particularly for smaller adjustments of the value, where the number of detected events would increase significantly. However, for increasing threshold values, the sensitivity diminishes, indicating that almost no events are detected regardless of further increases in the parameter. So, to avoid under-detection of removals by setting Condition B1. too high, and to focus on capturing only significant sharp drops, by not setting the value too low, the value of 15 cm was maintained. Condition B2. was less sensitive to changing threshold values, where only after a significant increase of the input parameter, the number of detected drops substantially grew.

The collection of the marked events from the signaling plots and their timestamps across the years, provided valuable insights into seasonal patterns when displayed. Additionally, the mean interval times between consecutive extraction events supported the findings on seasonal effects and a link between the occurrence of removals and the discharge behavior was found. Furthermore, the general method of detection and the conditions used for extraction marking, were validated against the logistical information on the operational procedure of the structure, as provided by the waterboard.

4.3. Extreme Value Analysis

Following the analysis of the water level difference across the trash rack through the detection method in Section 4.2.2, extreme modeling provided useful insights. A dataset of the identified extractions was created together with the corresponding values of the recorded sharp drops. From there, daily cumulative extreme values of sharp drop values were computed. This cumulative manner of extreme collection was instigated, because the real extreme behavior is naturally limited due to a system of periodic and threshold-triggered extractions. After the collection and accumulation of these extremes, further statistical analysis offered valuable information on the the frequency of occurrence of these extremes.

Extreme Value Analysis (EVA) is a useful, statistical tool used to model the extreme behavior of stochastic parameters, like the daily cumulative extremes in the case of this study. The statistical model most adequate for this research is the Peak over Threshold (PoT), given the continuous, non-stationary data and the focus on seasonal trends. It considers all individual exceedances of the extreme values above a specified threshold that occur within a day. According to the Pickands–Balkema–De Haan theorem, the selected extremes in the PoT method follow a Generalized Pareto Distribution (GPD) despite the parent distribution, which were used to construct the statistical model for this analysis.

With this statistical model, the probability of extreme events can be quantified through a return value plot. A return value plot allows for the estimation of return periods of events where large portions of debris are expected to be extracted from the structure in a single day. This is because the daily cumulative extreme is the stochastic parameter that is modeled. First, the return period for each observed extreme value is estimated as the inverse of the exceedance probability, calculated using its empirical cumulative distribution function (ECDF). By means of ranking the exceedances and normalizing them over the span of the dataset, these return periods can be derived. Subsequently, the GPD is fitted to the exceedances, allowing for return period estimation using the shape, scale, and location parameters. In Section 5.5 the EVA was conducted.

4.4. Application of the methods to other datasets

Following a thorough analysis of the Tungelroysebeek dataset, the detection methods, as described in Sections 4.2, were applied to the datasets of Uffelsebeek and Wanssum in Section 5.6 to test the applicability of the methods. Both datasets include discharge data and on-site water level measurements upstream and downstream of the trash rack, which makes the approach feasible. The EVA as described in Section 4.3 was not applied since the sample size was too small for an adequate analysis or unrealistic patterns in the collection of extremes arose. Besides, note that both later-obtained datasets are less reliable, as for smaller sites with smaller site dimensions and flow conditions, the same precision-instruments are present. Therefore, the discharge data are likely underestimated, and for Wanssum, the water level measurements can be corrupted. Despite these limitations, the two detection methods were applied to see whether similar results were obtained.

5 Results

5.1. Water level over time

During the exploration of Section 4.1, the sharp drops that suggested extractions of debris were detected in the Q-h measurements for Tungelroysebeek in 2010 in the months of November and December. After further investigation of the water level plots over time for other years, more instances of sharp drops were observed. So, given the continuous water level data, detection methods were developed that analyzed the water level time series for Tungelroysebeek and identify potential debris removals. To adequately mark these extraction events, a specific set of conditions were applied, these are listed and explained in Section 4.2.1.

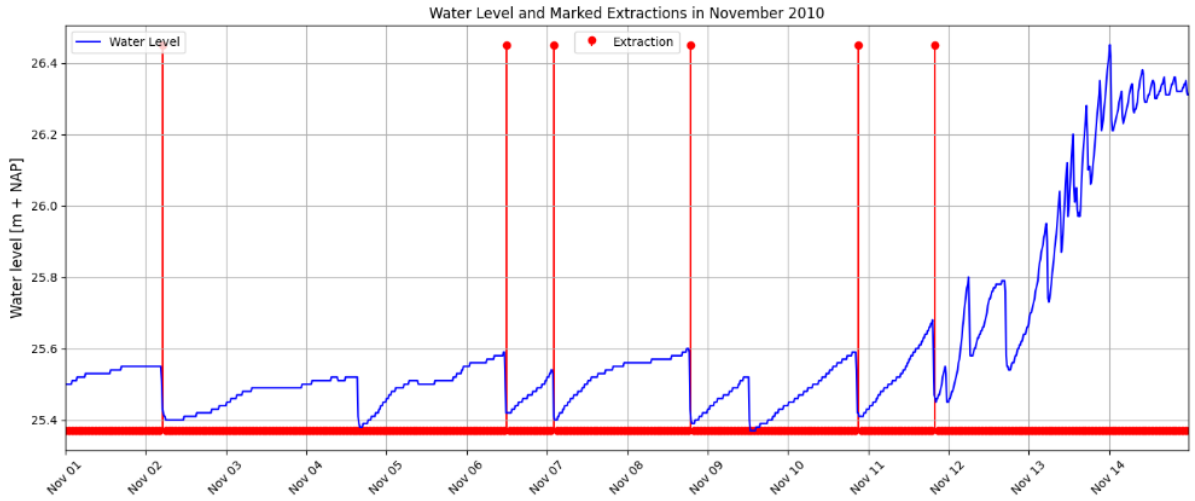

Figure 5.1: Water level and marked extractions at Tungelroysebeek in November 2010

Figure 5.1 shows the water level over time for Tungelroysebeek in the first two weeks of November 2010, with the sharp drops marked in red. the removal events were collected throughout the whole dataset and in Figure 5.2 a histogram is shown containing information on the monthly occurrences throughout the year together with the contributions of each year in the dataset. This plot shows the frequent occurrences of extractions during the fall, which complies with earlier remarks made in Section 4.1 and the waterboard's information. The inspector of the inverted siphon highlighted that the structure requires close monitoring during autumn due to falling leaves and branches, with additional cleaning sequences when needed. In addition to the sheddings of trees falling on the surface, elevated water levels and higher discharge also contribute to a higher frequency of occurrence in this period of the year. Yearly contributions appear to be distributed evenly, except for recent years, where the method detects almost no sharp drops. This could be due to a change in operational procedures which led to no significant sharp drops being detected in recent years.

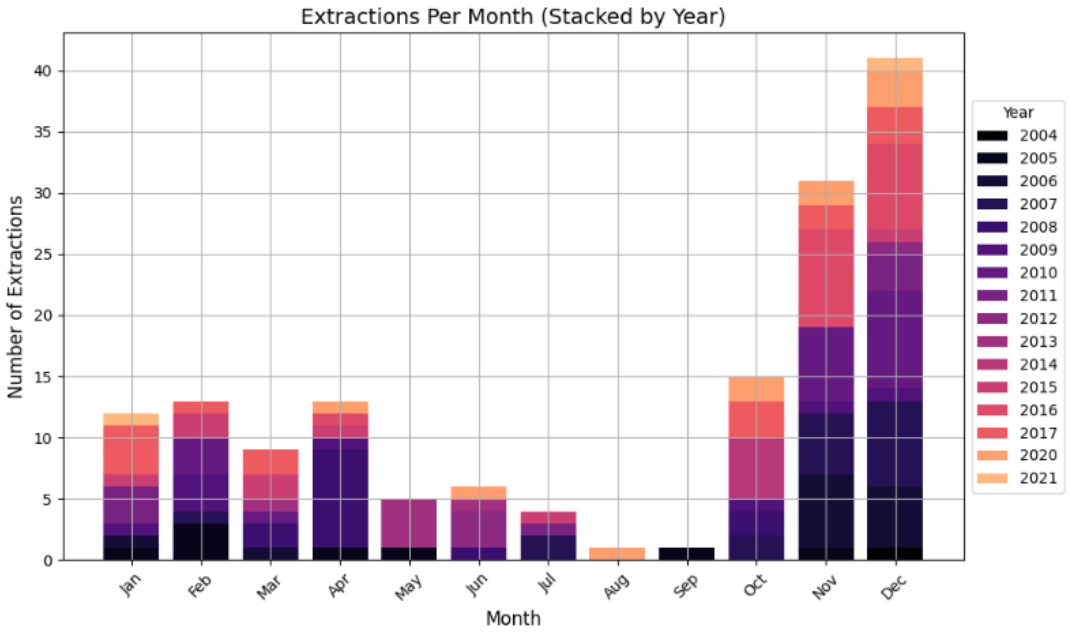

Figure 5.2: Extractions detected in water level plots collected across the years, displayed per month for Tungelroysebeek

It becomes evident from Figure 5.1 that not all events are captured. While the rises leading up to the drops appear to be gradual, it appears that some drops are not considered by the method, which could be due to the sensitivity of Condition A1. to changes of the input parameter, as can be seen in Appendix C. So, in general, this method tends to not fully represent the extraction behavior, since this procedure only relies on the upstream water level. The capturing of the removal behavior is limited as analysis of upstream water levels alone, overlooks the codependency of backwater rise and extraction conditions on the downstream water level. Additionally, the influence of the discharge is not taken into consideration in this detection method. So, it may be more insightful to develop a detection method that incorporates the interplay between up- and downstream water levels as well as the discharge's influence in setting the detection conditions. Therefore, an additional detection method was introduced.

5.2. Water level difference across the trash rack over time

In this second phase of identification of debris extractions, the analysis focuses on the course of the water level difference between upstream and downstream of the trash rack for the development of a second detection method. The water level difference across the trash rack for the first two weeks of November 2010 is plotted over time in Figure 5.3, alongside the identified extractions. This detection method identifies removal events if the water level difference upstream and downstream of the trash rack surpasses Condition B1., which is 15 cm and subsequently falls again below Condition B2., which is 5 cm. These conditions were elaborated on in Section 4.2.2.

Comparison of the two methods, at first sight, reveals that the second method more adequately captures the extraction behavior. For example, Figure 5.3 shows that for this period, the second method appears to mark all removal events as opposed to Figure 5.1, where some events are overlooked. Extending this hypothesis to the whole dataset, it was found that the second detection method more effectively captures the extraction behavior. For the first method, the condition selection only accounts for the behavior of upstream water levels, and contrary to the second method, neglects the influence of downstream water levels on the process of debris accumulation. Additionally, the influence of varying discharge was excluded in the first detection method where the second procedure accounts for the discharge's effects through the mean head loss.

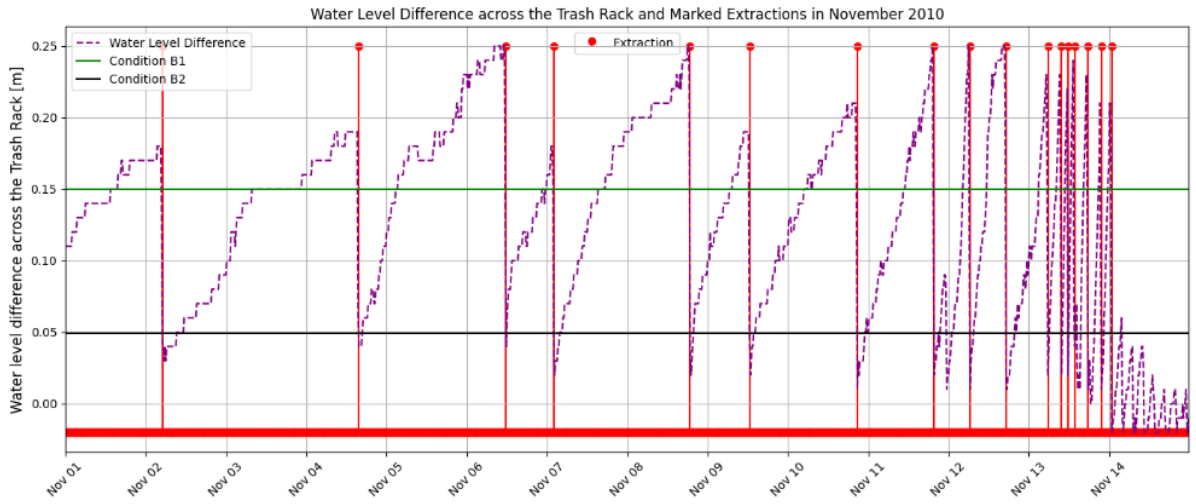

Figure 5.3: Water level difference across the trash rack and marked extractions, together with the detection conditions at Tungelroysebeek in November 2010

Additionally, analysis showed that a higher number of events were detected than the first method, because this second method provides a more comprehensive approach for the identification of the sharp drops. From reviewing the results of the second method it appeared that the earlier years between 2005 and 2011, have a significant contribution, approximately 60%, to the total detected sharp drops compared to more recent years. Possibly this is due to different operational methods used back then.

Collecting these instances and displaying them by means of a histogram with the extractions distributed over the months with the years' contribution visible, enables investigation of seasonal patterns. Figure 5.4 shows this histogram of the monthly occurrences and the yearly contributions of extraction events. Here, many extractions occur in the fall months, as was noted by the local inspector of the inverted siphon at Tungelroysebeek, where close monitoring and additional cleaning of the trash rack during this time of year is institutionalized. This observation in Figure 5.4 aligns with findings from the first method and is thus further supported by the information from the waterboard. It is evident from the figures that both methods reveal frequent sharp drops during November and December.

The inspector also noted that a cleaning sequence, automatically initiated by exceedance of the 35 cm threshold, rarely occurs, complying with the low number of values of the water difference across the trash rack higher than 35 cm found in the data. The accumulations were likely already removed upon inspection or by means of the daily sequence, before reaching the trigger value. Note also that both methods report almost no drops in August, likely since leaves and branches have not fallen yet and low flow conditions are expected.

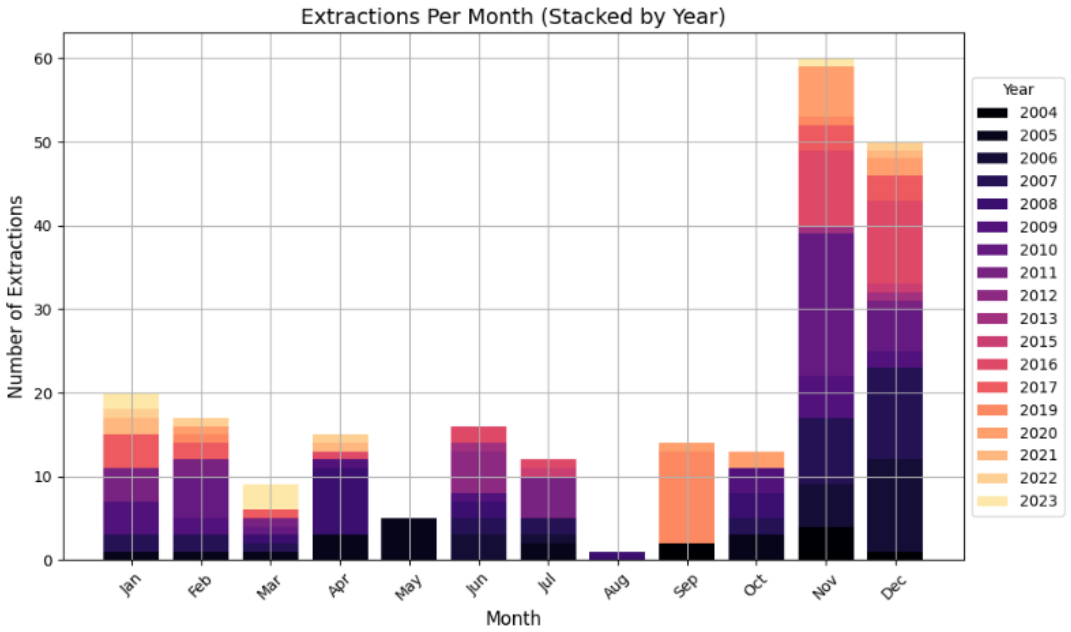

Figure 5.4: Extractions detected in water level difference across the trash rack, collected across the years, displayed per month for Tungelroysebeek

Besides, in Figure 5.3 it appears that the interval time between two extractions decreases throughout the course of days, leading to more frequent removals. To further reinforce this observation, a histogram showing the monthly mean interval between events and the total collected number of events per month across the dataset is presented in Figure 5.5. The figure highlights a seasonal pattern, with significantly more events and shorter intervals in the months of November and December. Moreover, in August it is evident that only 1 extraction is detected, therefore leading to a mean interval time of 31 days, and showing the seasonal influence of a summer month. Additionally, upon examining the plots of water level difference across the trash rack in combination with the available discharge data, it was observed that sharp drops more likely occur with increasing discharge values. In Section 5.3 this relationship will be further explored.

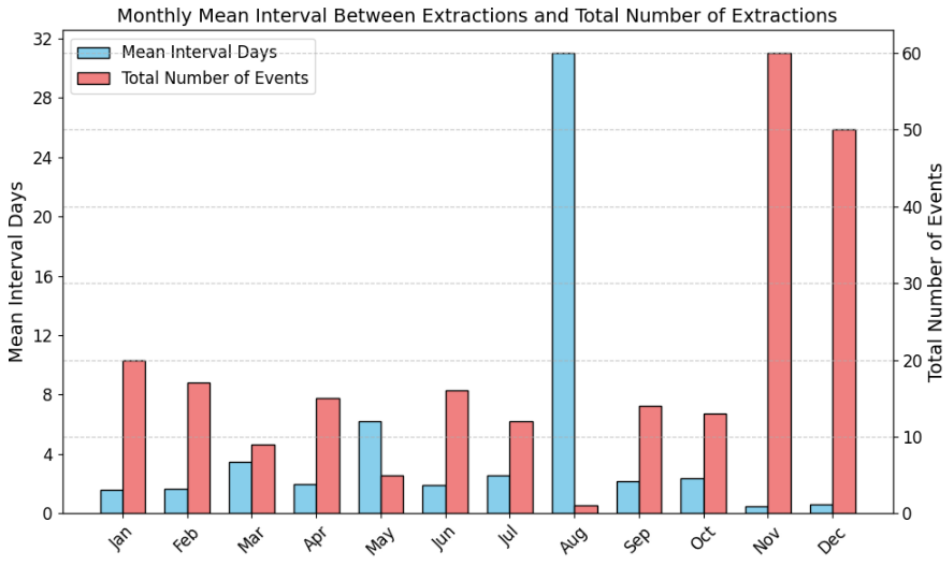

Figure 5.5: Mean interval time between extractions and total number of extractions per month at Tungelroysebeek

5.3. Relationship between extractions and discharge

It was noted that more sharp drops were recorded during periods of rising discharge, likely due to seasonally driven, increased flow conditions. With the collected sharp drops, representing extractions, the discharge behavior around these moments of removal was examined. For this analysis, it was essential that discharge data was present on the moment the sharp drop occurs, which was the case for approximately 38% of all data of water level differences across the trash rack. However, since discharge has been consistently recorded from 2021, and, as noted in Section 5.2, more recent years have a lower contribution of detected extractions, only 12.5% of all of sharp drops occurred at timestamps with simultaneous discharge recordings. Additionally, it was mentioned in Section 3.1 that the discharge is not measured independently and not directly at the structure. Despite these limitations, discharge behavior around sharp drops was analyzed.

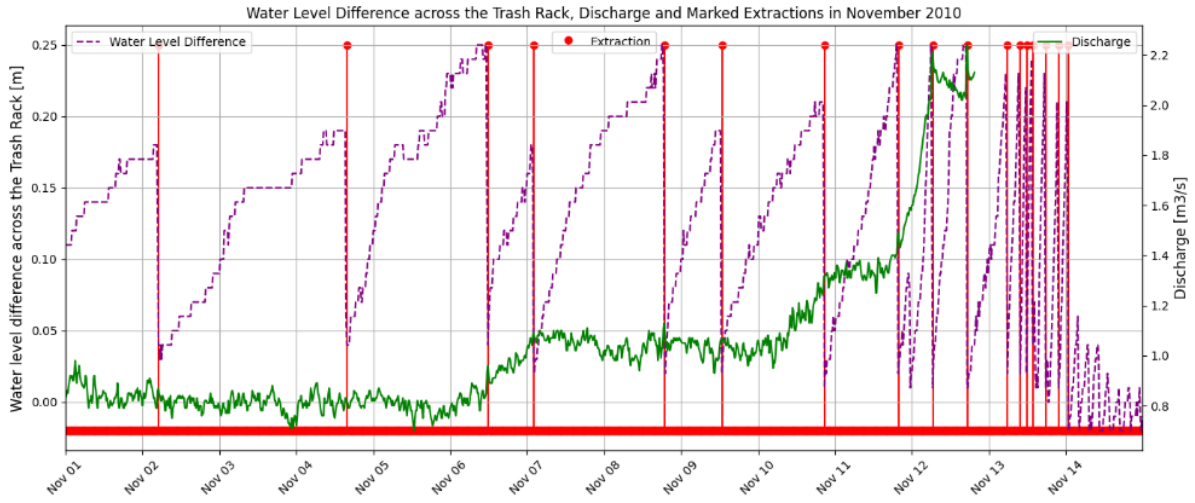

Figure 5.6: Water level difference across the trash rack alongside the discharge course at Tungelroysebeek in November 2011

During the first two weeks of November 2010 Figure 5.6 shows a significant increase of the number of sharp drops as discharge rises. Although discharge monitoring ceased after November 12th for unknown reasons, inspection of the data suggests that discharge likely continued to increase throughout the month. As for November 2010, the same observation can be made from Figure 5.7; a gradual, yet significant increase of discharge leads to the occurrence of three detected removals during the course of 2 days in January 2011, that have a higher magnitude than other extractions. This suggests a relationship between the rising discharge and size of the sharp drop value. Note that here the method failed to capture three extractions, that are seemingly significant but do not exceed Condition B1., and are therefore not collected by the method.

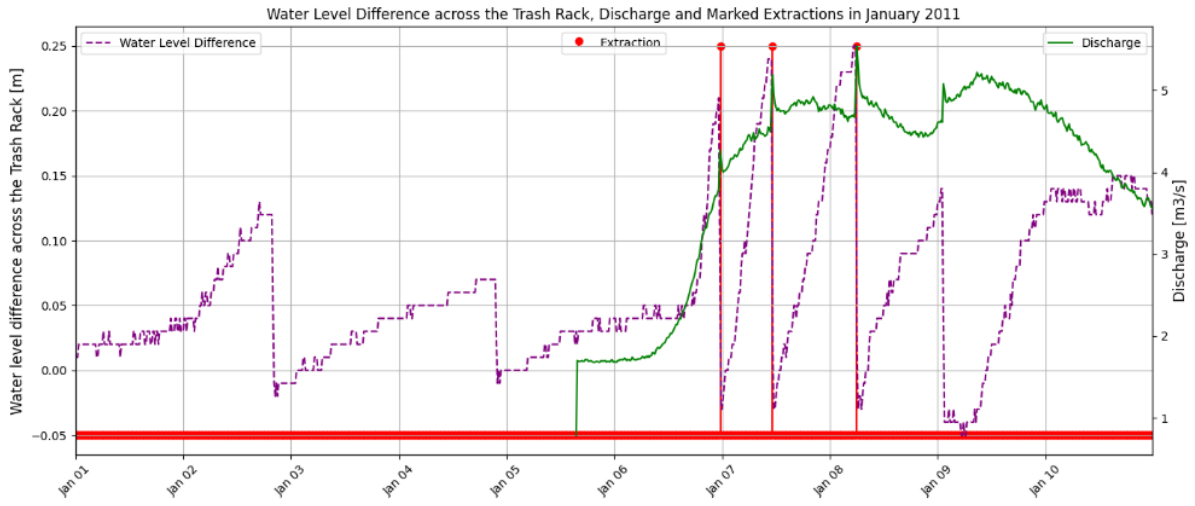

Figure 5.7: Water level difference across the trash rack alongside the discharge course at Tungelroysebeek in January 2011

In addition to steady increase in discharge leading to extractions, in Figure 5.8, as well as in Figure 5.7, a local peak was observed co-occurring with removals, which indicates a correlation between sudden discharge increases and extraction instances. Other plots of the water level difference across the trash rack alongside discharge behavior, where similar phenomena were observed, are provided in Appendix D.

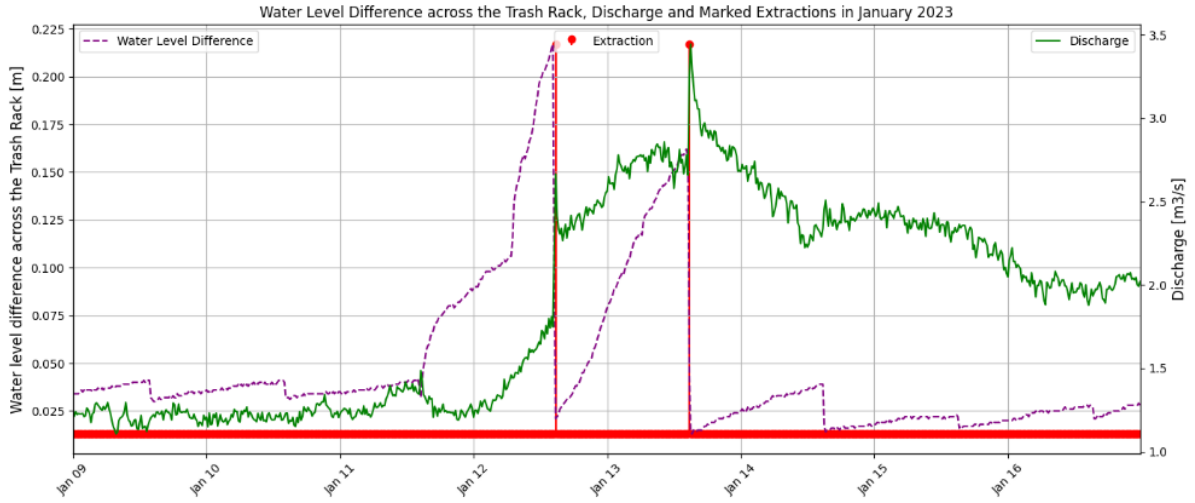

Figure 5.8: Water level difference across the trash rack alongside the discharge course at Tungelroysebeek in January 2023

An attempt was made to generalize this observation by plotting the magnitudes of the sharp drop values against their corresponding discharge values. However, since the availability of recorded discharge measurements during extractions was limited, this plot was not useful, as the results were of minimal quantity and too scattered for reasonable interpretations. Additionally, by analyzing the individual discharge course around the extractions another attempt was made to generalize the remarks made about gradual increase in discharge and observed peaks co-occurring with removal instances, however, displaying all individual discharge courses led to significant variability across events. This variability, combined with the limited number of detected extractions occurring simultaneously with discharge recordings, complicated the analysis of the discharge course around the moment of extraction and the influence it has on the magnitude of sharp drops.

5.4. Discussion of the operational procedure

Validation of the methods against the operating procedure, which consists of scheduled daily extractions at 11:30 and 23:30, removals triggered by threshold exceedance of 35 cm and upon inspection, is crucial to check the feasibility of the applied method. Based on the information received from the Waterboard, it would be expected that all captured cleaning events occur around noon and midnight, with additional instances corresponding to threshold exceedance or manual extraction. Figure 5.9 attempts to validate this by displaying the detected marked events as a function of the hour of the day. Nevertheless, the pattern of extractions, as indicated by the inspector, with a 12-hour period does not emerge from the bar plot. A peak can be observed before noon, possibly explained by the system not accounting for daylight savings, where in summer (GMT+2), scheduled extractions are reported at 10:30 but in actuality occur at 11:30, as the system measures water levels in GMT+1. However, this explanation does not clarify the absence of a midnight peak or the broad distribution of events throughout the day. Despite that inspector assured that the daily extraction procedure was active at least from 2017, these inconsistencies could stem from a shift in operational methods throughout the years, that did not rely on daily extractions for instance. Besides, inaccuracies in the data, or miscommunications with the waterboard, may have contributed to this misalignment.

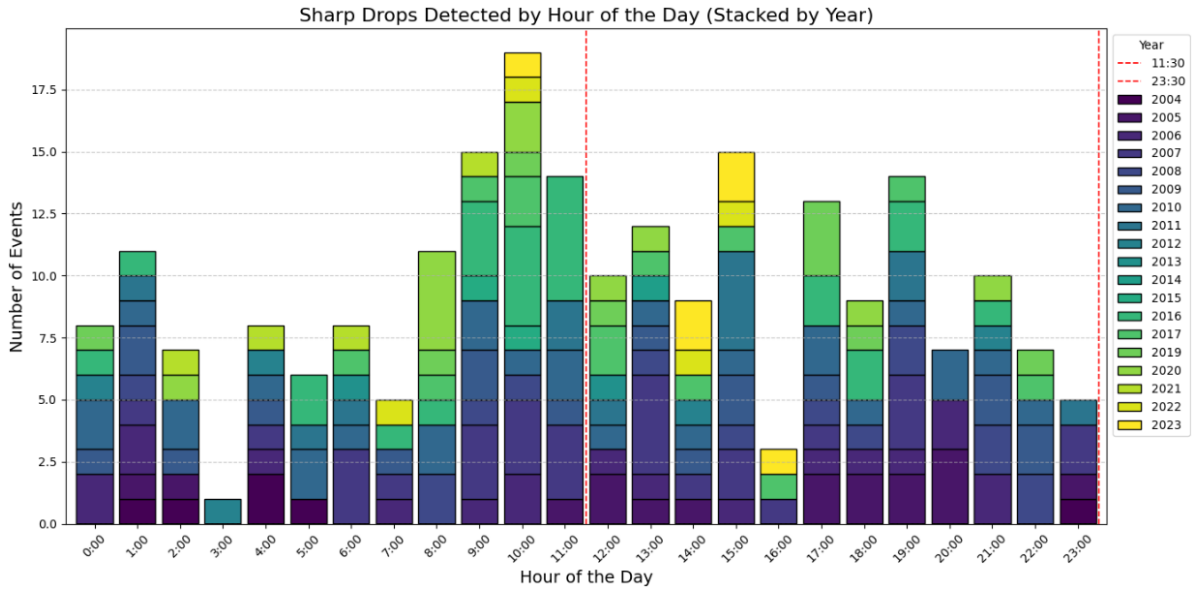

Figure 5.9: Histogram with detected extractions displayed by the hour of the day for Tungelroysebeek

Furthermore, although the moments of extraction do not always align with the waterboard's reported schedule, they still exhibit periodic behavior. For instance, in Figure 5.3, periodic removals are clearly noticeable, even though the marked instances in November 2010 do not occur at 11:30 and 23:30 with 12-hour periods. Similarly, more recently, Figure 5.10 displays the course of the water level difference across the trash rack over a week in January 2023, with vertical lines representing the scheduled removal times. This plot reveals that drops not only deviate from the scheduled times but also suggest a 24-hour interval between events. This deviation in cleaning period can also be seen from Figure 5.5, thus proving that the daily removal procedure as provided by Waterschap Limburg is not adequately reflected by the data. Furthermore, from the plot it becomes evident how the method struggles to capture insignificant removals.

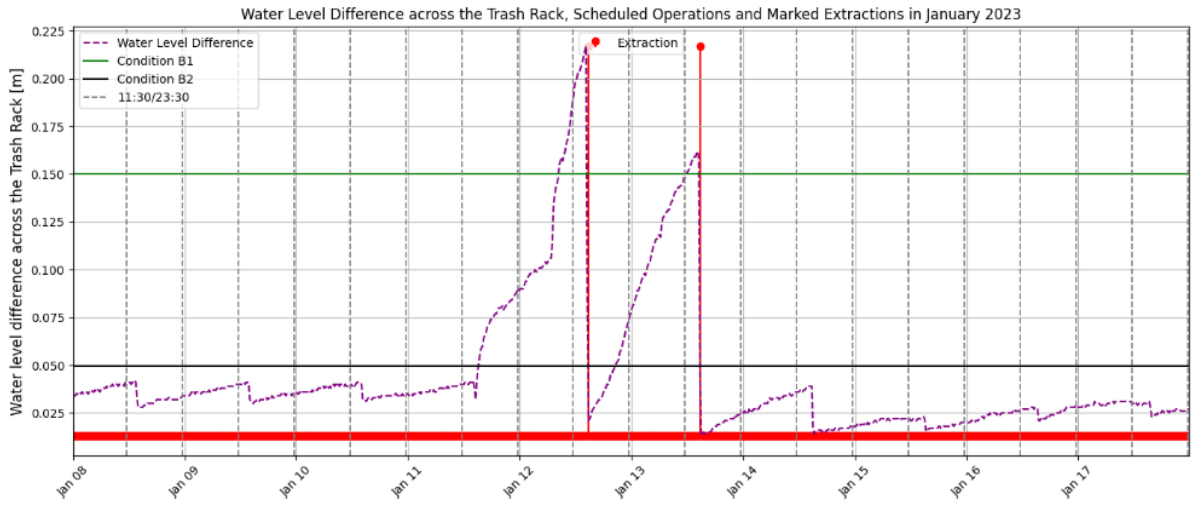

Figure 5.10: Water level difference across the trash rack and marked extractions, together with the detection conditions and daily scheduled removals for Tungelroysebeek in January 2023

5.5. Extreme Value Analysis

While some discrepancies exist on the validity of the operational procedure, Sections 5.1 and 5.2 provided reasonable insights on seasonal patterns for the occurrence of extractions. With the data on the sharp drops throughout the 20-year dataset obtained from Section 5.2, a statistical analysis on extreme water level difference values provided useful information on exceedance probabilities through return value plots. It was mentioned in Section 4.3 that as the stochastic variable, the daily cumulative extremes were used for the EVA. This strategy enables for the prediction of return periods of days where significant portions of debris are expected to be extracted from the structure. The return value plot is shown in Figure 5.11, where the observed values, as well as the fitted distribution, are plotted over their corresponding return periods. Additionally, for the 10 highest observed values, the number of accumulated extractions contributing to the total value is annotated alongside the marker of the observed value. Here it becomes evident that the highest observed values mostly coincide with a contribution of multiple extractions. Upon examining the lower values, a decline in number of accumulated extractions can be seen, but a full representation was omitted from the figure to maintain clarity.

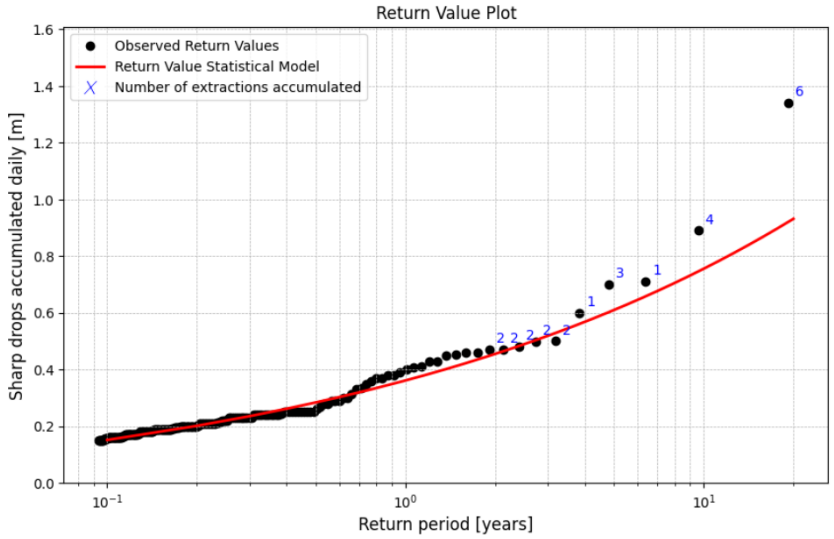

Figure 5.11: Return value plot with observed and modeled values of daily cumulative sharp drops and corresponding return periods

The model demonstrates a decent fit overall, however, struggles to accurately capture the tail behavior, which is due to the limited occurrence of significant cumulative extremes. This is challenging to account for in extreme value theory, and the fact that so many extraction events occur at the threshold, also influences the fit's attempts to represent the tail behavior. The plot indicates that for a return period of 10 years, a cumulative sharp drop value of approximately 75 cm can be expected; a significant value for this location.

A PoT-method was used to create the statistical model with a GPD applied. To evaluate the goodness of fit, a QQ-plot was generated in Figure 5.12, comparing the theoretical quantiles from the model with the observed quantiles. In an ideal fitted model, the quantiles are perfectly aligned in a 1:1-line. The figure shows a reasonable fit where occasionally the model over- or underestimates, although such deviations are difficult to eliminate entirely. It was particularly challenging to capture the two highest extremes.

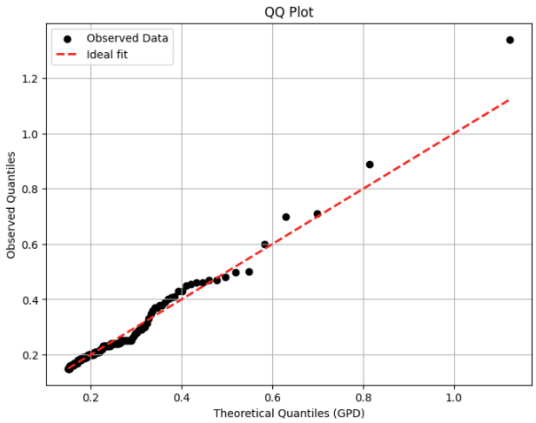

Figure 5.12: QQ-plot for the fitted distribution

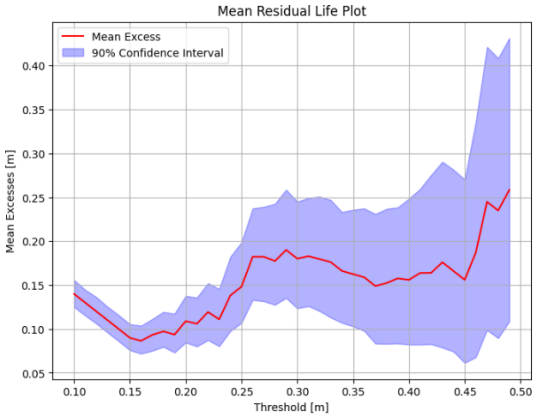

Figure 5.13: MRL-plot for PoT-threshold selection

For the threshold selection in the PoT-method, Condition B1. of 0.15 m, defined for removal detection in Section 5.2, was adopted, which is based on the mean head loss across the trash rack plus a margin. To further justify this selection, a Mean Residual Life (MRL) plot was generated, shown in Figure 5.13. This plot displays average excess values over a given threshold for a series of thresholds, and should exhibit a roughly linear trend beyond the selected threshold. The figure indicates that exceedance values are approximately linear between 0.15 m and 0.23 m, validating the selection. After this value, few excesses are collected, and therefore the sample size becomes too small for relevant analysis. However, it is important to note that for threshold selection, it is challenging to find a balance between bias and variance. Improving the statistical qualities of the model with a bigger sample size is induced by a lower threshold, and representing true extreme behavior is implied by a higher threshold. With too low thresholds, the tail is influenced by non-extremes being included, while too high thresholds result in few extremes being collected, thus a poor fit due to significant variance. In the case of this research, increasing the threshold led to high variance observed, and reducing the threshold further would contaminate the tail behavior.

The model underestimates the most extreme cases, which could potentially be resolved by incorporating more extensive datasets with more extreme occurrences, but it is a general challenge in extreme value theory that the occurrence of significant extremes is rare. Besides, overflowing or destruction of the measuring equipments poses additional potential difficulties. Additionally, the cumulative manner of extreme collection prevents the extremes to occur naturally. Finding a site where only threshold-triggered operations are scheduled, would provide a more reliable analysis and a more comprehensive statistical model.

5.6. Application of the methods to other datasets

Applying the established detection methods to the the later-obtained datasets of Uffelsebeek and Wanssum allows for testing the applicability of the procedures. This confirmed earlier, anticipated findings, and even though the reliability of these datasets can not be entirely ensured, as highlighted in Sections 3.5 and 3.6, subjecting them to the methods from Sections 5.1 and 5.2 still provided valuable insights. The same seasonal patterns with increased occurrences in fall months were observed in the data of both Uffelsebeek and Wanssum. The applied conditions for the established detection methods for the water level and water level difference across the trash rack are displayed in Table 5.1, where based on the values of the conditions, it can be seen that these sites are smaller and have lower flow conditions.

	First method			Second method	
	Condition A1.	Condition A2.	Condition A3.	Condition B1.	Condition B2.
Uffelsebeek	3 [cm]	10 [cm]	4 [cm]	10 [cm]	6 [cm]
Wanssum	10 [cm]	10 [cm]	4 [cm]	14 [cm]	3.7 [cm]

Table 5.1: Conditions applied for the detection of extractions for the methods from Sections 5.1 and 5.2

Here, Conditions A1., A2. and A3. for the first detection method pose thresholds for the size of the drop in water level, the rise of the water level preceding the extraction, and ensure that water level difference across the trash rack after extraction is approximately zero, respectively. A more detailed description can be found in Section 4.2.1. For the second method, Condition B1. was depicted by the mean head loss plus a margin representing clogged conditions. Together with Condition B2., defined by the mean head loss below which unobstructed flow was assumed, they pose the conditions for removal detection, as was shown in Section 4.2.2.

5.6.1. Uffelsebeek

Figures 5.14 and 5.15 show that the observed seasonal patterns from the analyses of the water levels and water level differences across the trash rack, align with findings from Sections 5.1 and 5.2 and information of Waterschap Limburg explaining the increased occurrences of extractions during the fall due to tree sheddings and elevated flow conditions. It shows that for the first method 2003 and 2004 appear to have a great contribution to the number of detected events. Note that for Tungelroysebeek and Wanssum, the second method proved to be a more comprehensive model leading to more detected sharp drops. As opposed to Uffelsebeek, where the first detection method more effectively captured the extraction behavior, most likely since for the second method, defining Condition B1. was challenging.

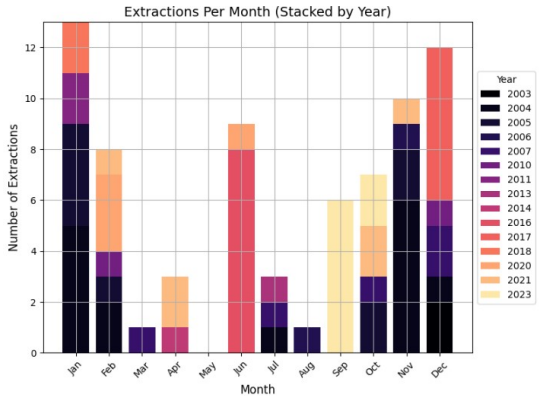

Figure 5.14: Extractions detected in water level plots collected across the years, displayed per month for Uffelsebeek

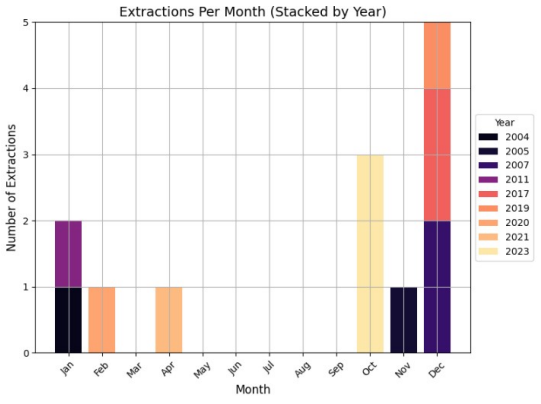

Figure 5.15: Extractions detected in water level difference across the trash rack, collected across the years, displayed per month for Uffelsebeek

It should be noted that Condition B2., corresponding to a computed mean head loss of 3 cm in the second method, was manually increased to capture more removal events. However, even favorably adjusting the condition, did not result in detecting more events, which is surprising given the size of the dataset. This could be associated with the small site where smaller fluctuations and lower extremes occur, complicating the detection process due to the same error margins applied to the instruments.

5.6.2. Wanssum

For Wanssum, the same autumn-induced increase of occurrences in the fall and winter months was observed. This is displayed in Figures 5.16 and 5.17, further reinforcing previous insights. Notable is the significantly high number of removals detected in the second method, despite the smaller size of the dataset. The sensitivity of Condition B1. resulted in capturing many events. Furthermore, 2022 seems to have great contribution to the detection of sharp drops for both methods, and the reason that this is not seen at the other datasets, might be due to the fact that the sites are relatively far from each other and therefore experience different patterns in flow conditions, while Tungelroysebeek and Uffelsebeek are located in relatively close proximity.

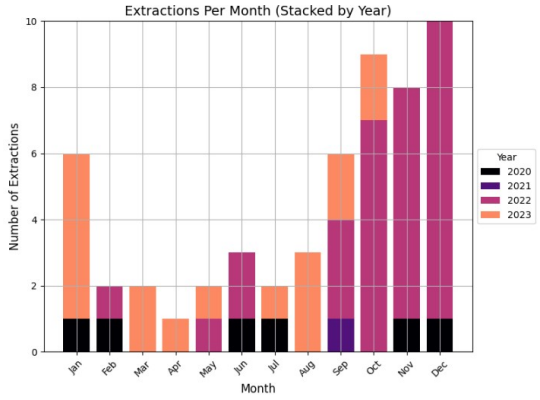

Figure 5.16: Extractions detected in water level plots collected across the years, displayed per month for Wanssum

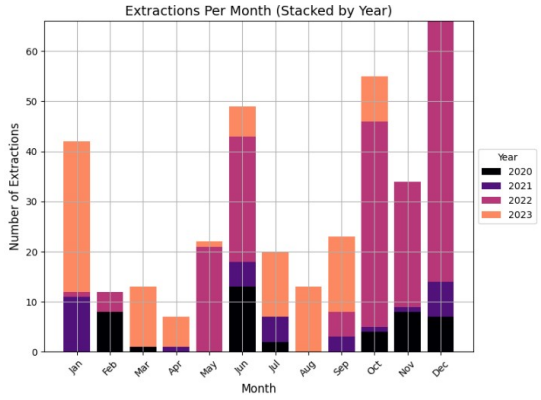

Figure 5.17: Extractions detected in water level difference across the trash rack, collected across the years, displayed per month for Wanssum

After examination of the data, it was observed that the water level differences across the trash rack significantly exceeding Condition B1. of 14 cm rarely occurs. This results in an abrupt decline in number of events detected as the threshold values increase in the sensitivity analysis in Appendix C.3. Conditon B2. is not significantly influenced by the selection of higher values, only smaller ones.

5.6.3. Detection sensitivity

Exploring the water level variations over time and collecting the detected extraction events over the year displayed similar, anticipated seasonal effects. However, defining the conditions that rely on the mean head loss over the trash rack, was particularly challenging. Accuracy of the instruments and discharge being measured at significant distance resulted in high sensitivity observed in the conditions for the detection methods. Comparing the sensitivity analyses, that are included in Appendix C.2 and C.3, with Tungelroysebeek, similar patterns are revealed, though with varying degrees of sensitivity. The selected conditions for the first detection method displayed similar degrees of sensitivity, where adjustment of the parameter value results in similar numbers of detected events. However, the set of conditions for the second method exhibited substantially more sensitivity than for Tungelroysebeek and showed the need for careful selection. For instance, at both sites, Condition B1. and B2. showed notable sensitivity to changes of the input variable for the second detection method. Low values for Condition B1. and high values for Condition B2. resulted detection of a significant number of sharp drops. Whereas, the number of detected sharp drops reduced remarkably for higher values of Condition B1. and lower values of Condition B2.. This suggests that significant sharp drops rarely occur. Overall, the sensitivity of the conditions across sites highlights the need for careful calibration and the use of accurate instruments to optimize event detection.

5.7. Summary

This research phase provided interesting findings, but it also brought up uncertainties linked to the operational procedure of these structures. Seasonal patterns on the occurrences of debris extraction were evident for both detection methods throughout the years at the sites of Tungelroysebeek, Uffelsebeek and Wanssum, and confirmed anticipated assumptions. The obtained findings corresponded with information from the waterboard that the increased number of extractions in autumn months is due to the accumulation of fallen leaves and branches, along with elevated flow conditions typical of this season. This was also highlighted by the plots in Section 5.3. Furthermore, the EVA on the daily cumulative extremes showed a reasonable fit, and enabled for return period estimation for days where large portions of debris are expected to be removed from the trash rack upstream of the inverted siphon of Tungelroysebeek. However, it also exhibited challenges regarding underestimation of the tail due to the rare occurrence of critical extremes.

At the same time however, attempts to align the detected markings with operational removal procedures revealed inconsistencies in the timestamps and intervals between extraction events. Examination of the water level differences across the trash rack over time based on the marked events resulted in uncertainties about the applied methods, the instruments' precision and potential changes in operational procedure over the years. Furthermore, application of the detection methods to other datasets led to coinciding results. However, challenges also arose in setting the detection conditions and high sensitivity was observed of the applied conditions for extraction detection.

6

Discussion

6.1. Reflection on the approach

6.1.1. Q-h analysis

The examination of the Q-h measurements proved to be useful for the analysis as it led to identifying sharp drops in the water level. Debris-induced anomalies were observed where the water level rose and fell, for a discharge that remained more or less constant. This was explained by blockage of debris causing the water level to rise, and removals causing the drops. The analysis showed that Q-h measurements can be used to detect debris-induced irregularities in the flow regime for broader, scientific applications. However, challenges also emerged when determining whether the observed anomalies were induced by debris accumulation, or other potential causes. Operational proceedings or malfunctioning the equipment can result in observing anomalies that are not necessarily debris-related, and therefore, one should carefully assess other possible causes. Additionally, the use of precise measurements would improve the reliability of the analysis. Section 6.2 reflects upon this more in depth.

Furthermore, utilizing more continuous discharge data, would result in a more complete representation of the yearly flow conditions and lead to a more comprehensive strategy for the detection of debris accumulation. Similarly, attempts to link the discharge to the occurrence of extractions in Section 5.3 would benefit greatly from continuous discharge data. It would allow for displaying the relationship between the magnitude of the sharp drop in the water level difference across the trash rack, which could offer insights on the influence of Froude number on the extracted amounts of debris. Erpicum et al. [2023] and Burghardt et al. [2024] noted that increased backwater rise is caused by higher Froude numbers and lower initial water depths, whereas this research showed that the significant sharp drops are observed with increasing discharge. While these observations do not contradict each other, determining whether an increase in discharge locally corresponds to a higher Froude number, or if significant extractions consistently correspond with increased backwater rise, depends on multiple factors. Future research should validate these findings by utilizing datasets with more complete discharge data and linking marked extractions to measurable debris properties, such as mass or volume. This could offer opportunities for coupling debris management strategies to expected flow conditions, and therefore enhance predictive modeling. Despite these challenges, analyzing discharge variations during significant extractions offered valuable insights into how flow conditions influence debris accumulation.

6.1.2. Debris detection methods

The developed detection methods enabled the identification of debris extractions by analyzing the water levels and water level differences across the trash rack and marking the removals driven by observed anomalies in the Q-h measurements. Both methods detected an increase in extraction occurrences during autumn, particularly in November and December, aligning with remarks made by the inspector of the inverted siphon. This seasonal pattern suggests that operational debris removal is influenced by meteorological and hydrological conditions, reinforcing the need for seasonally adaptive detection methods and monitoring strategies.

However, the application also uncovered challenges in setting the detection conditions, where high sensitivity was observed. Refining the detection conditions through adaptive modeling and deploying high-precision instruments would enhance detection accuracy, enabling a more comprehensive capturing of the removal behavior. For the first method from Section 5.1 that identified extractions in the water level, incorporating the influence of the downstream water level and discharge would contribute to a more extensive detection method. While the second detection method from Section 5.2, based on the water level differences across the trash rack, was more comprehensive, it still faced challenges detecting smaller extractions, due to the rigid set of detection conditions that relied only on a mean head loss value which was computed with the mean flow velocities. Incorporating a flexible set of conditions that account for monthly flow variations would improve detection reliability.

Moreover, aligning the collected removal events with operational information from the waterboard revealed some inconsistencies regarding extraction timing. This underscores the importance of a well-calibrated method with operational procedures. Additionally, upon examination of histograms of the detected extractions across the dataset for both methods, a low contribution of recent years was observed, possibly due to a shift in operational procedures. In future works, adjusting the detection methods accurately to the historical operations, could prevent uncertainties. Regardless of these limitations, the detection methods provide valuable insights into seasonal debris removal trends. Their application to historical datasets demonstrates their potential for advancing debris research and improving monitoring strategies. These insights could support real-time monitoring systems for anticipating debris accumulation events, where incorporating seasonal accumulation trends into predictive flood models could improve risk assessments in debris-prone waterways.

In addition to the two detection methods that assess the water level variations, an attempt was made to utilize the grid loss factors in combination with the continuity equation for the detection of debris. Deviating values from the validated grid loss factors would be an indication of debris presence. Blockage by debris accumulation in addition to existing blockage due to the trash rack, would translate into observing higher grid loss factors. This can also be derived in Equation 2.15, that takes into account the blockage ratios of the trash rack and the debris accumulation. However, the results from this analysis reported unrealistic values and were therefore not included. To refine such a detection method, accuracy of the measuring instruments needs improvement for assessment of the water levels and calculation of the head loss over the trash rack. Moreover, more precise flow velocity and discharge measurements on-site would provide more consistent results, since the method was highly sensitive to fluctuations in the flow velocity in the siphon, which affected the head loss computation. The use of accurate and reliable water level and discharge data is crucial for proper application of this proposed method and for obtaining useful results. Section 6.2 further discloses this requirement.

6.1.3. Extreme Value Analysis

After identifying the extractions, a statistical model was introduced through the EVA in Section 5.5 that allowed for return period estimation for debris accumulation. The results from this analysis provide valuable insights for flood-risk assessment and predictive modeling. By assigning a return period to the occurrence of debris accumulation improved flood-risk management strategies can be developed at inverted siphons equipped with trash racks. The statistical model showed a good fit but underestimated the tail of the distribution. The considered stochastic parameter was a daily accumulation of sharp drops in the water level difference across the trash rack. From the return value plot it was evident that the highest two observed extremes coincided with the contribution of multiple extractions on the same day. This observation highlights how it was challenging for the statistical model to fit the distribution of observed extremes, due to the daily accumulation procedure limiting the natural occurrence of extremes. This potentially contributed to the model's underestimation of the tail of the distribution.

This analysis provided a useful tool for estimating the likelihood of days with significant debris extractions. However, this method does not allow for the quantification of the volume or mass of debris which is expected to arrive. Incorporating methods to use measurable parameters, like volume or mass of debris, for the EVA, would provide more quantifiable insights on debris-induced extreme behavior. In addition, when attempting to apply EVA to the later-obtained datasets, it was emphasized that the method of daily cumulative extremes collection requires careful consideration and might not be applicable to all datasets. Using a site that allows for direct assessment of individual extreme events instead of accumulating them daily, would enhance the reliability of the EVA, since the occurrence of extreme debris accumulations would follow a more natural process. Despite these challenges, this approach offers a framework for assessing debris-related flood risks and provides optimization efforts for further research on extreme behavior of debris accumulations.

Proper threshold selection is crucial for obtaining reliable predictions in EVA, as it directly influences statistical precision and the accuracy of extreme event modeling. There is always a trade-off between increasing the sample size by setting a lower threshold in the PoT-method, thus increasing the statistical properties, and representing the true tail behavior by setting a high threshold. This trade-off of variance and bias emphasizes that the selection of the threshold is a careful process, and that it should be taken into consideration for improving future efforts in performing EVA on debris accumulation processes. In this analysis it was found that with an increase of the threshold, the quality of the statistical model degraded significantly. A similar limitation was observed also in attempts to apply the EVA to the later-obtained datasets, where the need for sufficient sample-size of extremes was underscored. In contrast, efforts to generate confidence bounds by means of bootstrapping highlighted the importance for utilizing a dataset containing true extremes. Bootstrapping is a resampling method that propagates variability of the data into the variability of the fitted parameters, and since the occurrence of critical extremes was rare, uncertainties were amplified when creating the confidence intervals, especially for critical extremes. The concentration of lower extremes can introduce a bias by including non-extremes in the distribution. This underscores the precise consideration when selecting thresholds for the PoT-method, and shows how methods like the MRL plot can facilitate these decisions.

6.1.4. Application to other datasets

Testing the established detection methods to the datasets of Uffelsebeek and Wanssum confirmed their applicability, as similar seasonal trends were observed, but also revealed challenges constructing the detection conditions, where high sensitivity was observed. This was likely due to the accuracy of the measuring equipment in combination with the smaller size of the sites, which posed challenges to capture the smaller fluctuations with the same precision as the instruments at Tungelroysebeek. Additionally, the distance of the discharge measuring instrument and additional inflow by other creeks, led to a potentially underestimated discharge for the computation of head loss. Furthermore, the EVA was not applied to these last two datasets. For Uffelsebeek, this was due to the low number of detected events that limited the sample size significantly, which led to a poorly fitted statistical model. For Wanssum, the rare occurrence of significant exceedances complicated the EVA. Additionally, sharp drop values clustering around multiples of the exceedance threshold due to the daily accumulation procedure, led to unrealistic patterns in the extreme collection. This underscored the importance of employing reliable datasets of sufficient size to conduct an EVA.

6.2. Instrument accuracy and datasets

The results provide valuable insights on development of detection methods for debris accumulation through analysis of water level and discharge datasets, where seasonal effects were observed and extreme behavior was modeled. However, the limited precision of the measuring equipment of 2 cm per sensor, so 4 cm in total for the two instruments presented challenges. Initial exploration of the Q-h measurements, accurately capturing removal events and modeling of the extreme occurrences were limited. For instance, it complicated the calibration of the extraction detection methods in Sections 5.1 and 5.2 as the set of rigid detection conditions occasionally did not reflect the actual presence or absence of debris accumulations. Minimizing the error margin by deployment of more accurate monitoring equipment, would avoid sharp drops in the water level variations to fall within this range of error and improve the methods' detection ability. Similarly, for EVA, where the model used a dataset of collected extremes to fit a distribution, improving accuracy would enhance the reliability of the results.

Moreover, when developing methods that employ the mean head loss for detection of debris accumulations and extractions of debris, the need for reliable discharge measurements is highlighted. This research utilized discharge data that is occasionally measured at a significant distance and influenced by additional flows from smaller creeks and waterways. Additionally, the discharge values are derived through flow velocity and water depth measurements. Uncertainties in the discharge data transitioned into challenges computing the head loss values and setting the detection conditions. Therefore, implementing discharge data that is derived from flow velocities measured directly at the structure's site, would significantly improve the effectivity of the detection method. The analysis of the Q-h measurements, which relies on both accurate water level and discharge data, would also benefit greatly from this.

Despite the challenges, this study demonstrates that analysis of Q-h measurements, application of detection methods and EVA can provide valuable insights into seasonal debris accumulation. These findings suggest that real-time monitoring systems could integrate seasonal trends and insights on extreme accumulation behavior to optimize maintenance strategies. Future work should focus on improving measurement precision and expanding datasets to refine management strategies and predictive models for hydraulic structures equipped with trash racks in flood-prone areas.

7

Conclusions and Recommendations

7.1. Conclusions

Backwater rise at inverted siphons and submerged culverts, caused by debris-induced blockages, can exacerbate inundation risks and result in significant damages. Previous research on this topic primarily focused on laboratory experiments examining the local effects of debris or retrospective analyses inventorying debris compositions and potentially associated damages. In contrast, this thesis researched the opportunities of utilizing on-site measurement data for the detection of debris accumulations and extractions at trash racks upstream of inverted siphons in Limburg. The objective was to explore and develop methods for identifying debris removals in the provided, historical datasets containing water level and discharge data. Deploying these methods and collecting the instances of debris extraction, provides an enhanced understanding of seasonal effects on and extreme behavior of debris accumulation processes. This focus led to the formulation of the first research question as follows.

Can debris accumulations at inverted siphons be detected, utilizing on-site water level and discharge data?

Detecting debris accumulations at trash racks upstream of inverted siphons or submerged culverts can be done by combining insights from an analysis of the Q-h measurements and development of debris detection methods. Direct detection of debris accumulations from the annual Q-h measurements of Tungelroysebeek and Bunde proved to be challenging. However, a detailed examination revealed promising debris-induced anomalies, occurring as sharp drops in the water level, that suggested extractions of debris. Identifying these sharp drops provided a methodology for exploring debris accumulation events in the corresponding water level variations of Tungelroysebeek. The analysis of Q-h measurements served as a valuable preliminary tool for identifying debris-related anomalies. They established a foundation for more targeted detection methods that analyze water level behavior and water level differences across the trash rack. These detection methods consisted of defining specific conditions to identify and mark removal events. The first method analyzed water levels over time, while the second was applied to water level differences across the trash rack, which proved to more effectively capture the extractions. Even though disparities arose in representing the full removal behavior, application of these methods offered opportunities in detection of debris accumulation in discharge and water level data. This was further supported by applying the methods on the datasets of Uffelsebeek and Wanssum and obtaining similar results. Application of the detection methods and collecting the removal instances enabled obtaining a deeper insight into the seasonal influences, which led to the formulation of the following research question.

What are the seasonal effects on debris accumulation processes, and how are they portrayed in the data?

To effectively demonstrate the seasonal effects on the occurrence of debris accumulation, the recorded removal events from the two detection methods were collected throughout the year with the months' contribution displayed in a histogram. Mapping the extractions revealed a significant increase in removal occurrences during the fall months, especially in November and December. This is likely due to the shedding of leaves and branches, in combination with elevated flow conditions typical for that time of year. This observation aligns with the information from the inspector of the inverted siphon, who underscored the need for extra monitoring and additional cleaning in autumn. Furthermore, mean interval time between extractions was inversely related to the number of detected extractions per month, where, again, in November and December many events were detected with shorter interval times. Finally, the seasonal influence on debris accumulation processes was confirmed by displaying the collected removal events from the later-obtained datasets, where similar seasonal patterns were observed. So, with the extractions identified by the detection methods and the seasonal effects uncovered, examining the extreme behavior of debris accumulation provided a deeper understanding of extreme behavior in accumulation processes.

How can extreme behavior in debris accumulations be demonstrated, and what is the frequency of occurrence?

For assessing the extreme behavior of debris accumulation, fitting a statistical model to observed extremes proved to be useful. This approach allowed for analyzing the frequency of occurrence of debris extractions, and offered opportunities for quantifying the probability of occurrence of extreme events by attributing a distribution. By performing an EVA, return periods were estimated for days at which significant portions of debris are expected to be extracted from the structure. To account for the scheduled daily removal procedure, the values for the detected sharp drops from the second method were accumulated per day. Overall, the model showed a good fit, however it struggled to represent the critical extremes resulting in underestimation the tail of the distribution. Additionally, finding the balance in setting the threshold for the events to be considered extremes, was proven to be challenging. However, the domain of the performing an EVA on debris accumulations and extractions was underexplored, and this research has proven that it is possible to identify a relationship between debris accumulation and return periods by means of statistical modeling. In the future, the use of higher-quality, extensive historical data would better facilitate the analyses of extreme debris accumulation events.

Overall, this thesis provides methods for detecting debris presence through analysis of datasets with on-site water level and discharge measurements. Further understanding of seasonal effects and extreme behavior of debris accumulation can support engineers in design and mitigation measures for the debris management and predictive modeling at hydraulic structures equipped with trash racks. Moreover, this research provides insights on debris accumulation processes that can be useful for future flood-risk assessment. To improve further studies on this topic, the following recommendations are proposed based on the findings and limitations outlined in this research.

7.2. Recommendations

Relying on data, where the discharge and water levels are measured at the same location, rather than Q-h measurements from different locations, would provide a more accurate representation of the flow conditions on site. Furthermore, consistently utilizing well-calibrated, high-precision instruments is essential for improving the effectivity of the applied analyses. This approach would improve the precision of the Q-h analysis for anomaly detection, thus leading to more accurate identification strategies. It would also result in more reliable values for the conditions used in debris extraction detection methods, where smaller extractions can be more easily identified. Additionally, this would allow detection methods that use the grid loss factor to be further explored. For the EVA, utilizing longer datasets of higher quality would increase the sample size of collected extremes and therefore enhance the statistical qualities without corrupting the true tail behavior.

Providing a more flexible set of detection conditions, would improve the adaptivity of the methods. More adequately representing the different flow conditions throughout the year, would increase the reliability of the outcomes and alignment with operational information. A recommendation to achieve this would be to combine insights from both detection methods. By implementing a framework of conditions that identifies extractions in the water level difference across the trash rack through imposing thresholds on the magnitude of the drop, the rise preceding the drop and a clean trash rack after extraction. Values for these conditions should be appointed by the value of the moving average of the head loss per month. This would lead to a more adaptive detection method that could capture the monthly differences of the water level across the trash rack more comprehensively. Moreover, incorporating an accurate representation of both current and historical operational procedures and site-specific parameters into model configurations, would improve the reliability of the analyses. Consulting time series of the extraction cycles reported by the waterboard would allow for validation of the methods' detection outcomes. Additionally, making use of a power graph of the extraction crane, would allow for estimating quantities of removed debris based on the amount of energy used per extraction.

Furthermore, by identifying debris extractions in historical datasets, this research solely looks at the consequences; the removals of debris, and overlooks the cause; the actual accumulation process. Introducing cameras on site facing the trash rack would provide an in-depth insight to the accumulation process and lead to drawing more reliable conclusions. Additionally would it allow for the validation of the applied methods through continuous image or video acquisition. This would be particularly valuable for verifying events like debris accumulation, extraction instances, and extreme occurrences. Using captured visual data to develop machine learning models focused on object detection and instance segmentation, could offer innovative techniques for validating detection procedures and potentially enabling quantification methods. Installing additional cameras facing the pile where the extraction crane dumps the removed debris could provide further insights. When combining these images with power graphs, this approach could offer new opportunities for quantification of debris volumes or mass.

Lastly, for Waterschap Limburg, deploying higher precision instruments for operational procedures that are triggered after a lower water level differences across the trash rack, could enhance maintenance planning. Thus potentially preventing the occurrence of critical accumulation events. Further recording and storing the extraction cycles' time series, would improve the detection methods' validity. Furthermore, integrating insights on seasonal effects and extreme occurrence into improved food-management strategies could help mitigate potential blockages that increase flood risk.

Bibliography

Abeling, S. (2022). De Geulduiker onder het Julianakanaal. L1 Nieuws.

Bayón, A., Valero, D., and Franca, M. J. (2024). Urban flood drifters (UFD): Identification, classification and characterisation. *Journal of Flood Risk Management*, 17(3).

Bocchiola, D., Rulli, M. C., and Rosso, R. (2008). A flume experiment on the formation of wood jams in rivers. *Water Resources Research*, 44(2).

Burghardt, L., Poppema, D., L., B., Wütrich, D., Erpicum, S., and Klopries, E. (2024). Multi-lab investigation of the effect of debris composition on bridge clogging during floods. 10th International Symposium on Hydraulic Structures Zürich, Switzerland.

De Jong, J. and Asselman, N. (2022). Analyse overstromingen Geulmonding. Technical report, Deltares.

Erpicum, S., Benet, L., Burghardt, L., Klopries, E., Poppema, D., and Wüthrich, D. (2023). Data collection, modelling and prediction. Technical report, RWTH Aachen University, TU Delft, Liège University.

Herschy, R. W. (2009). *Streamflow Measurement*. CRC Press, 3rd edition.

Honingh, D., Van Emmerik, T., Uijttewaal, W., Kardhana, H., Hoes, O., and Van De Giesen, N. (2020). Urban River Water Level Increase Through Plastic Waste Accumulation at a Rack Structure. *Frontiers in earth science*, 8.

Kataoka, T. and Nihei, Y. (2020). Quantification of floating riverine macro-debris transport using an image processing approach. *Scientific Reports*, 10(1).

Kirschmer, O. (1928). *Untersuchungen über den Verlust an Rechen bei schräger Zuströmung*. Mitteilungen Hydraulisches Institut München.

Koks, E., Van Ginkel, K., Van Marle, M., and Lemnitzer, A. (2022). Brief communication: Critical infrastructure impacts of the 2021 mid-July western European flood event. *Natural hazards and earth system sciences (Print)*, 22(12):3831–3838.

Korswagen, P. A., Harish, S., Oetjen, J., and Wüthrich, D. (2022). Evaluation of building damage during the July 2021 flash-flood in the Ahr Valley (Germany). Technical report, EGU General Assembly 2023, Vienna, Austria.

Lyn, D., Cooper, T., and Condon, C. (2007). Factors in Debris Accumulation at Bridge Piers. Technical report, Purdue university.

Lyn, D., Cooper, T., and Yi, Y.-K. (2003). Debris Accumulation at Bridge Crossings: Laboratory and Field Studies. Technical report, Purdue university.

Meusberger, H. (2002). Energieverlusten an Einlaufrechen von Flusskraftwerken. Technical report, Versuchsanstalt für Wasserbau Hydrologie und Glaziologie der Eidgenössischen Technischen Hochschule Zürich.

Mohr, S., Ehret, U., Kunz, M., Ludwig, P., Caldas-Álvarez, A., Daniell, J., Ehmele, F., Feldmann, H., Franca, M. J., Gattke, C., Hundhausen, M., Knippertz, P., Küpfer, K., Mühr, B., Pinto, J. G., Quinting, J., Schäfer, A., Scheibel, M., Seidel, F., and Wisotzky, C. (2023). A multi-disciplinary analysis of the exceptional flood event of July 2021 in central Europe – Part 1: Event description and analysis. *Natural hazards and earth system sciences (Print)*, 23(2):525–551.

Muste, M., Ho, H.-c., and Kim, D. (2010). Considerations on direct stream flow measurements using video imagery: Outlook and research needs. *Journal of Hydro-environment Research*, 5(4):289–300.

Panici, D. and De Almeida, G. A. M. (2018). Formation, Growth, and Failure of Debris Jams at Bridge Piers. *Water Resources Research*, 54(9):6226–6241.

PDOK (2024). Waterschappen Oppervlaktewateren IMWA.

Rantz, S. E. (1982). Measurement and Computation of Streamflow: Volume 2. Computation of Discharge. Technical report, U.S. Geological Survey.

Rijkswaterstaat (2021). Stroomgebiedbeheerplan Maas 2016-2021. Technical report.

Rijkswaterstaat (2024). Waterinfo - national water management information. Accessed: 2024-11-01.

Roggenkamp, T. and Herget, J. (2024). Flood reconstruction – The unexpected rather frequent event at River Ahr in July 2021. *Global and Planetary Change*, 240:104541.

Ronckers, D. (2022). Hydraulic behaviour of the Geul inverted siphon: energy losses, debris accumulation and applicability of a Minimum Energy Loss culvert. Technical report, Technische Universteit Delft.

Ronckers, D. (2024). Effects of driftwood on backwater rise at submerged culverts. Technical report, Technische Universteit Delft.

Ronckers, D., Poppema, D., and Wütrich, D. (2024). Experimental study on driftwood accumulation at submerged culverts. Technical report, TU Delft.

Schalko, I. (2018). Modeling Hazards Related to Large Wood in Rivers.

Schalko, I., Schmocker, L., Weitbrecht, V., and Boes, R. M. (2019). Laboratory study on wood accumulation probability at bridge piers. *Journal of Hydraulic Research*, 58(4):566–581.

Schall, J. D., Thompson, P. L., Zerges, S. M., Kilgore, R. T., and Morris, J. L. (2012). Hydraulic Design of Highway Culverts, Third Edition. *U.S. Department of Transportation Federal Highway Administration*.

Schmocker, L. and Hager, W. H. (2011). Probability of Drift Blockage at Bridge Decks. *Journal of Hydraulic Engineering*, 137(4):470–479.

Shashi Menon, E. (2015). *Transmission Pipeline Calculations and Simulations Manual*. Gulf Professional Publishing.

Tullis, B. P. (2012). *Hydraulic Loss Coefficients for Culverts*. The National Academies Press.

van Heeringen, K., Asselman, N., Beersma, J., Overeem, A., and Philip, S. (2022). Analyse overstroming Valkenburg. Technical report, Deltares.

Voorendt, M. and Molenaar, W. (2021). *Manual Hydraulic Structures*. TU Delft.

waterschap Overmaas en Roer (2016). Waterstanden en Afvoeren.

Wyss, A., Schalko, I., and Weitbrecht, V. (2021). Field Study on Wood Accumulation at a Bridge Pier. *Water*, 13(18):2475.

zuiveringschap Limburg (2002). Meerjarenrapport Waterkwaliteit Limburgse Oppervlaktewateren. Technical report, Waterschap Limburg.

A

Overview of the inverted siphons

A.1. Tungelroysebeek

The inverted siphon is fully submerged and consists of 3 pipes with a diameter of 1.65 meter and a heart-to-heart distance of 3.30 meters. It has a total length of approximately 91 meters. In Figure A.1, a technical drawing side profile of the structure is shown. Furthermore, in Figure A.2 the inverted siphon is shown in on the general area map, together with the bottom elevations upstream and downstream of the structure, provided by Waterschap Limburg. The width of the creek upstream and downstream was estimated to be 10 meters.

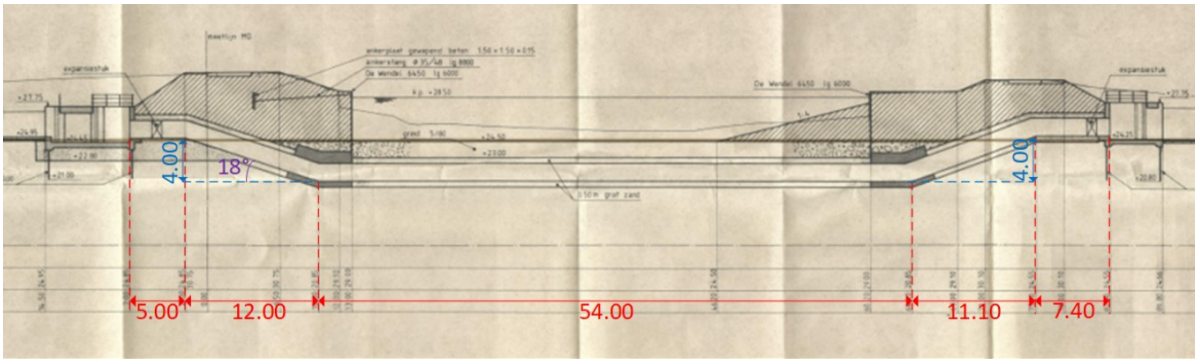

Figure A.1: Side profile of the inverted siphon in the Tungelroysebeek, Ronckers [2024]

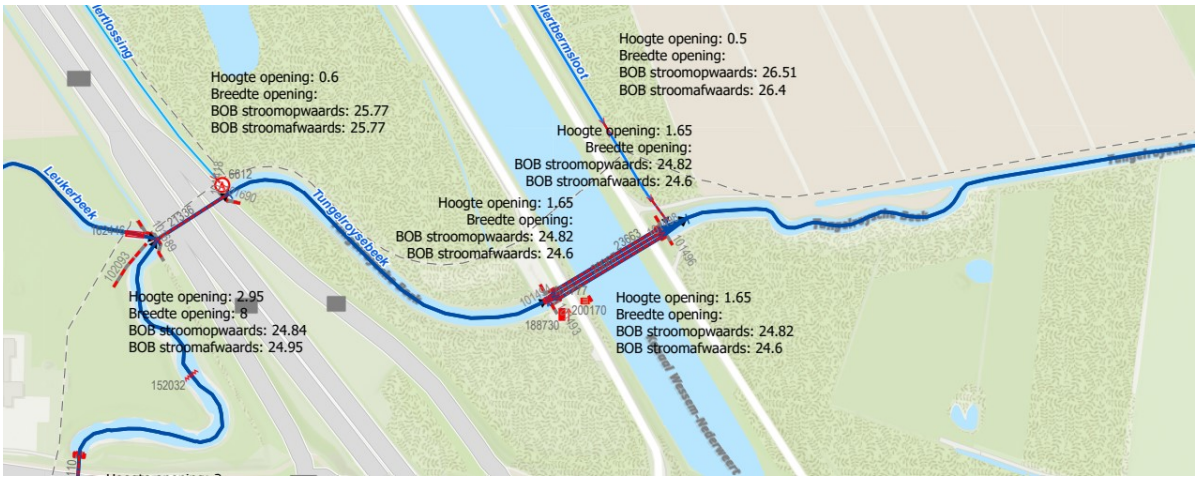

Figure A.2: Area map of the inverted siphon in the Tungelroysebeek

A.2. Bunde

The inverted siphon at the Bunde site consists of 5 squared conduits of 2.5 meters wide and high, including walls of 20 centimeters in between. Figures A.3 and A.4 provide technical drawings of the side and front profiles of the inverted siphon.

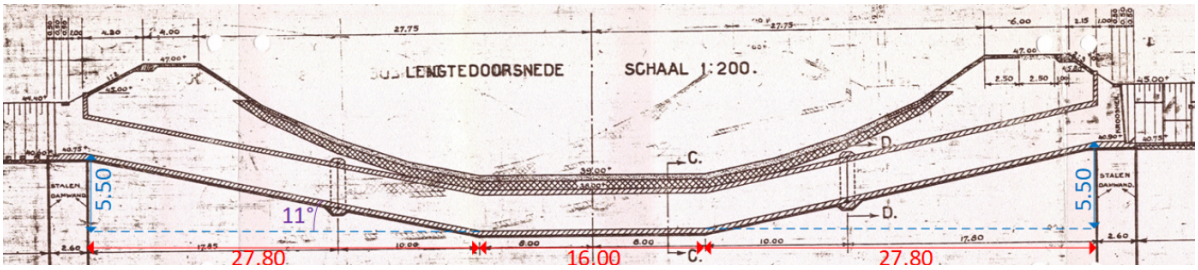

Figure A.3: Side profile of the inverted siphon in the Geul at Bunde, Ronckers [2024]

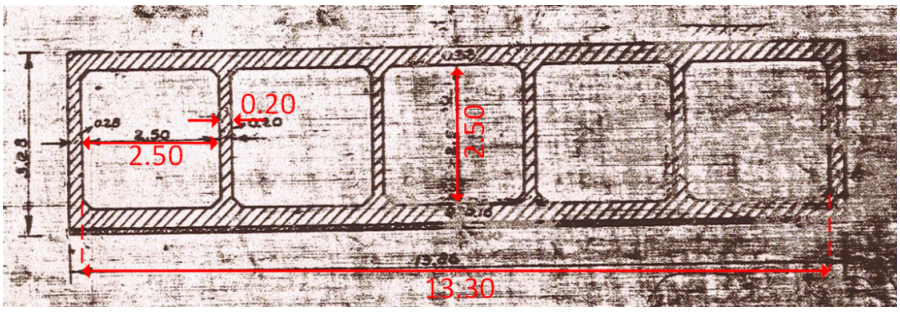

Figure A.4: Front profile of the inverted siphon in the Geul at Bunde, Ronckers [2024]

A.3. Uffelsebeek

The structure in the Uffelsebeek has similar longitudinal dimensions as the one in the Tungelroysebeek because they convey a waterway under the same Wessem-Nederweert Canal. It consists of two pipes with a 1.75 meter diameter. Figure A.5 shows the area map including the bottom elevations, provided by Waterschap Limburg.

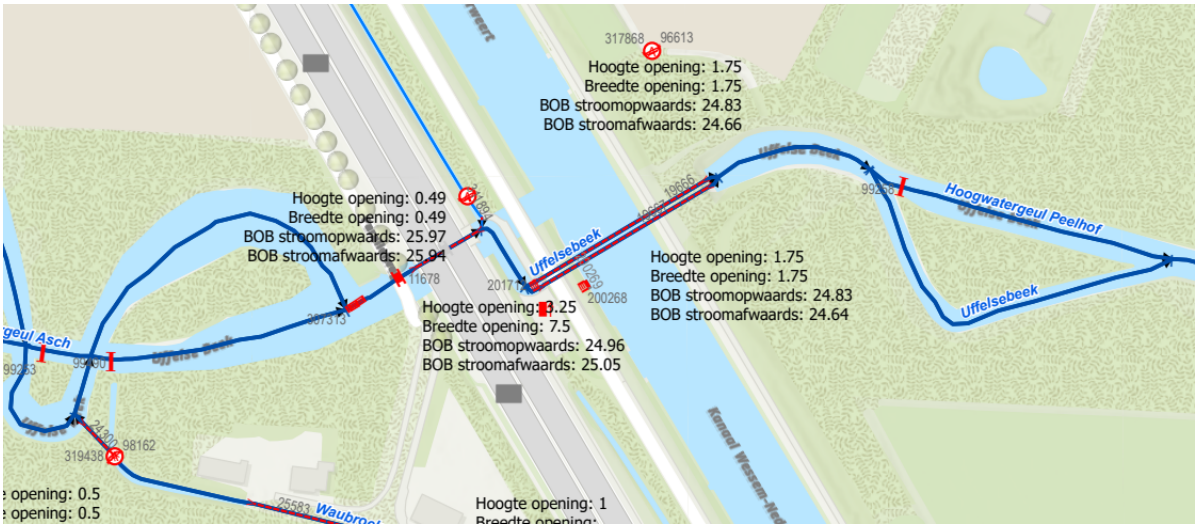

Figure A.5: Area map of the inverted siphon in the Uffelsebeek

B

Other anomalies in the Q-h measurements

B.1. Hysteresis

Analyzing the Q-h measurements for both Tungelroysebeek and Bunde, revealed recurring hysteresis patterns in the behavior of the Q-h measurements over several-day periods, as depicted schematically in Figure B.1. It seems like the Q-h measurements follows a trajectory where the water level rises and falls again, and at certain discharge values, multiple water level values can be read. See for instance Figure B.2, which displays the Q-h measurements of February 2011 for Tungelroysebeek.

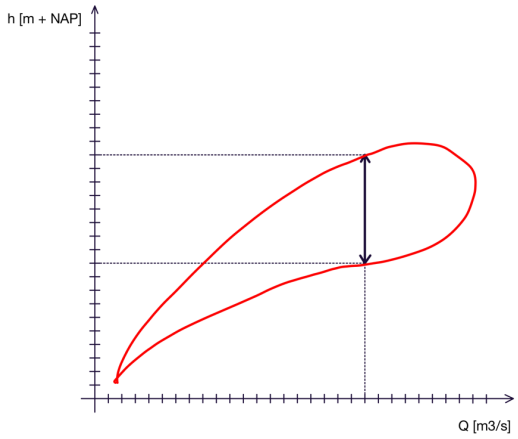

Figure B.1: Graphical representation of hysteresis in Q-h measurements

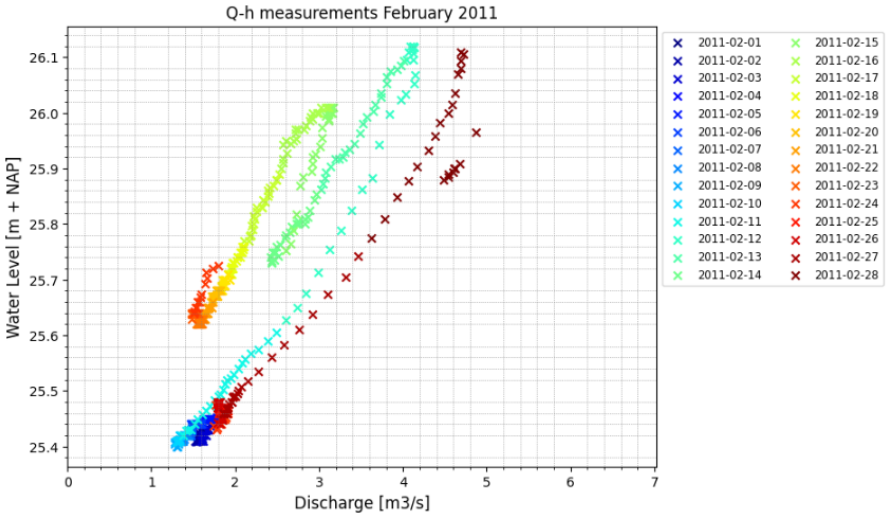

Figure B.2: Q-h measurements at Tungelroysebeek in February 2011

When observing these hysteresis instances, one is reminded of the double-sided loop in Q-h measurements by Muste et al. [2010] as discussed in Section 2.6, which exhibit similar hysteresis-like occurrences. However this link can be ruled out since this occurs over the course of a passing flood wave, and the perceived hysteresis from the data occurs over the course of multiple days.

The 2021 Q-h measurements at Bunde highlights notable occurrences in July, coinciding with the 2021 flooding event. As shown in Figure B.3, hysteresis is evident from July 13th to 18th, during the start of heavy rainfall in South Limburg, De Jong and Asselman [2022]. The first discharge peak occurred on July 15th, with water levels in the Meuse and Geul peaking on July 16th. However, due to data corruption at the upstream station from July 15th onward, further analysis of this event was discontinued.

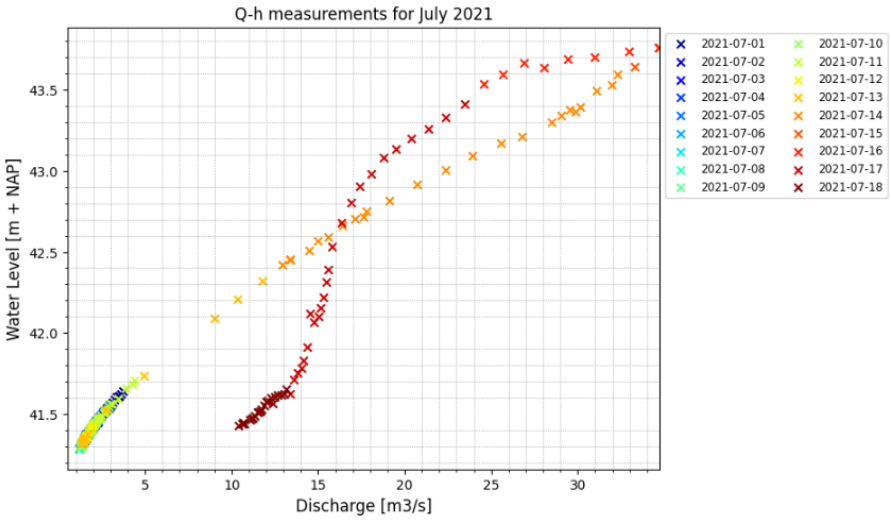

Figure B.3: Q-h measurements at Bunde in July 2021

B.2. Two trends

The last anomaly that was observed occurred in the Q-h measurements for the first half of the year 2024 at Bunde. Based on Figure B.4 it seems like there exist two trends depicting the nature of the flow, where the first three months show higher water levels and the months April and May seem to have higher discharges occasionally. The difference in the slope of the Q-h measurements is particularly striking. The presence of a few days with higher discharge during the spring months could be a result of wet spring conditions with substantial precipitation. Another reason, could be the opening or closing of one of the gates, based off of the seasonal conditions.

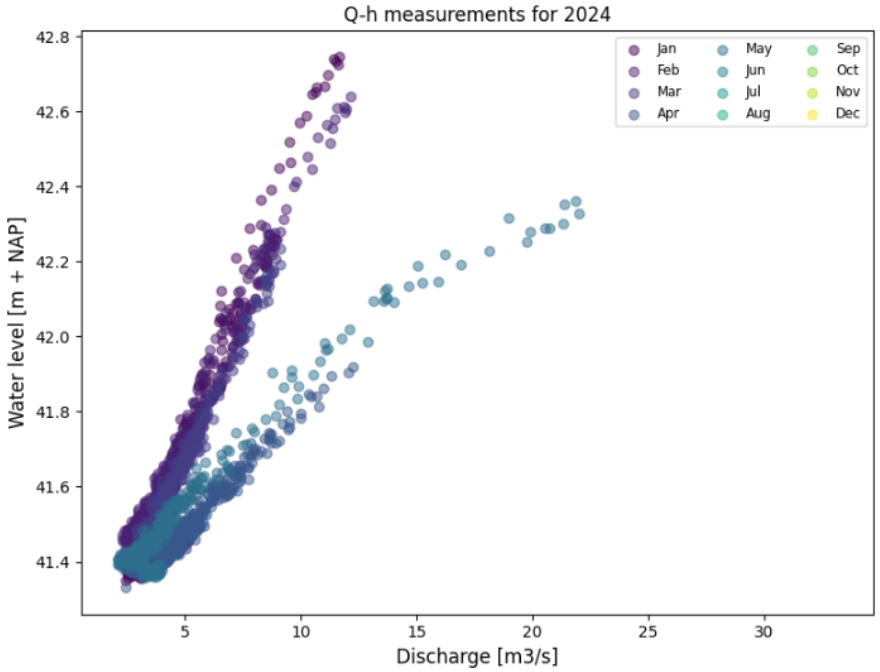

Figure B.4: Q-h measurements at Bunde in 2024

B.3. Summary

Among all observed anomalies, the sharp drops in water levels stand out as the most promising focus for further investigation, since they can be linked with debris accumulations, which aligns the objectives of this study. For the other two cases, the presence of debris accumulation is not apparent in the Q-h measurements. Hysteresis was observed over the course of multiple days and the trend behavior covered months even, whereas accumulating debris most likely occurs over the course of hours. At Tungelroysebeek, the daily extraction procedure, rules out the involvement of these cases at clogging of the inverted siphon. Furthermore, if a genuine difference in trend was present at Bunde, a similar phenomenon would be expected in the 2024 Q-h measurements of Tungelroysebeek. Therefore, these two additional anomalies were left out of the report.

C

Sensitivity Analysis

The sensitivity analysis evaluates the method by testing a range of parameters and analyzing their impact on outcomes. For the two methods highlighted in Chapter 5, combinations of conditions were applied, and the number of detected events was counted. This provides a visual representation of parameter sensitivity through plots, highlighting the trade-offs between detecting more events and maintaining reliability.

C.1. Tungelroysebeek

The sensitivity plot in Figure C.1 displays an almost exponential-like behavior, steepening near Condition A1., indicating high sensitivity to small changes. Yet, this condition was maintained to ensure the collected drops were significant without capturing minor water level deviations. The plot in Figure C.2 appears not so sensitive around Condition A2., with higher values no longer resulting in more detected events. Conditon A3. displays some sensitivity, but since it represents the accuracy of the measurement equipment, it is unreasonable to change this value according to its sensitivity to changes.

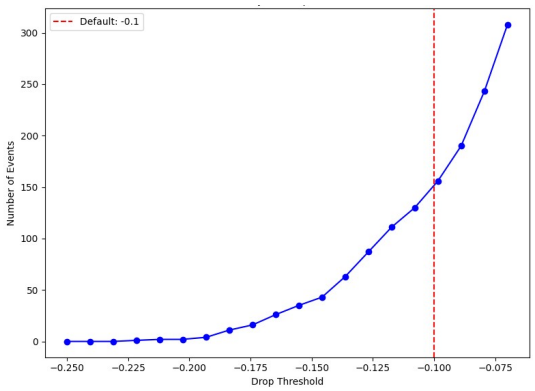

Figure C.1: Sensitivity of Condition A1., Tungelroysebeek

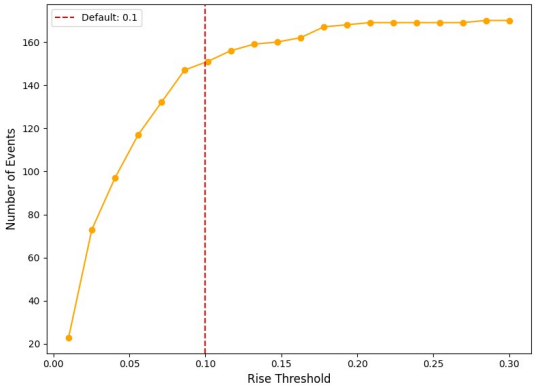

Figure C.2: Sensitivity of Condition A2., Tungelroysebeek

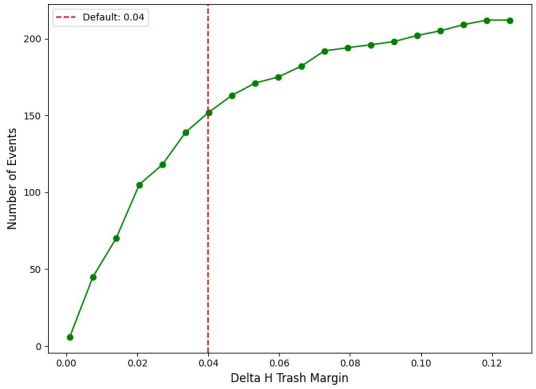

Figure C.3: Sensitivity of Condition A3., Tungelroysebeek

In Figure C.4, lower values for Conditon B1. captured more events, likely including less significant fluctuations, while higher values excluded such cases, focusing on significant drops in the stage difference. The selected condition of 15 cm aimed to balance excluding insignificant fluctuations while still detecting everyday removals. Conditon B2., in Figure C.5, increased steadily until a sharp rise was observed. This condition was retained as it represents the mean head loss, below which, clean rack conditions are suggested.

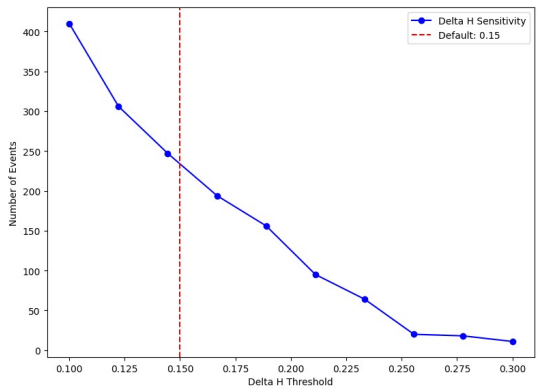

Figure C.4: Sensitivity of Conditon B1., Tungelroysebeek

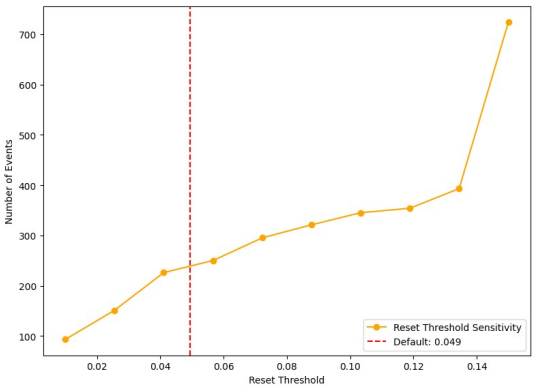

Figure C.5: Sensitivity of Condition B2., Tungelroysebeek

C.2. Uffelsebeek

The sensitivity plots show similar patterns as the Tungelroysebeek, but the conditions exhibit more sensitivity to changes. Condition A1. of 0.03 m in Figure C.6 seems reasonable for capturing significant events without including too many minor changes, but further lowering of this value leads to significant increase of detected events. Condition A2. is not sensitive to changes around 0.1 m, as shown in Figure C.7. Condition A3., in Figure C.8, shows less sensitivity to changes in close proximity to 0.04 m.

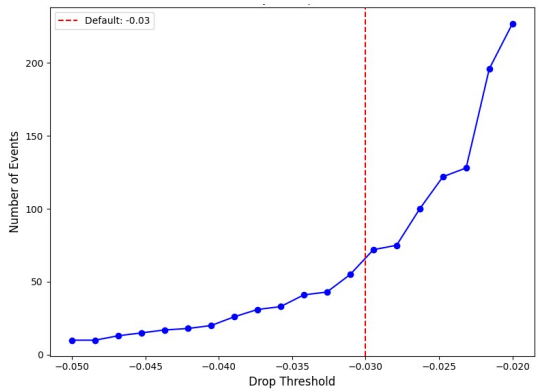

Figure C.6: Sensitivity of Condition A1., Uffelsebeek

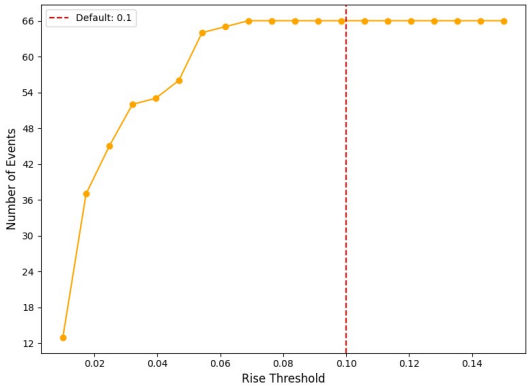

Figure C.7: Sensitivity of Condition A2., Uffelsebeek

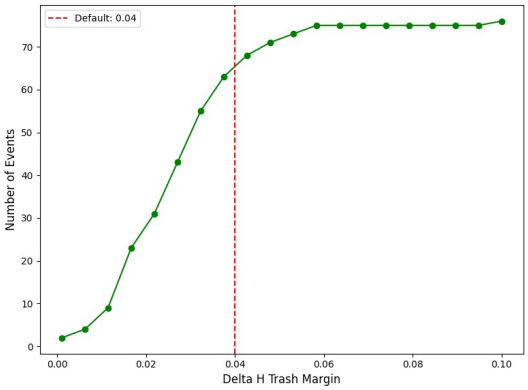

Figure C.8: Sensitivity of Condition A3., Uffelsebeek

Both Conditon B1. and B2. show that a low number of events is expected for the selected values with low sensitivity around that value. They are displayed in Figure C.9 and C.10 respectfully. Both figures clearly show how sensitive the two thresholds can be for low values of Conditon B1. and high values for Conditon B2.. Here, Conditon B1. below 0.07 m, or Conditon B2. above 0.08 m, would lead to sharp increase of number of events.

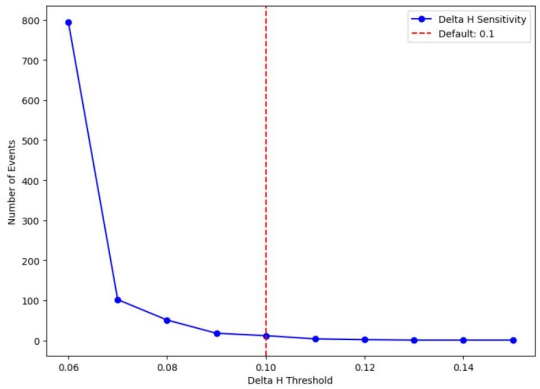

Figure C.9: Sensitivity of Conditon B1., Uffelsebeek

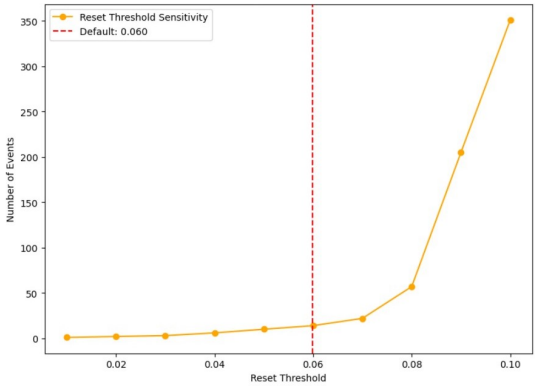

Figure C.10: Sensitivity of Condition B2., Uffelsebeek

C.3. Wanssum

Similarly for Uffelsebeek and Tungelsebeek, the conditions show similar patterns of sensitivity. Condition A1. in Figure C.11, shows that less negative values lead to a steeper rise of number of events than the other sites, but the condition is selected right before the sharp increase of recorded events. Figure C.12 shows that Condition A2. is not further influenced by higher values of the parameter. This goes for Conditon A3. as well in Figure C.13.

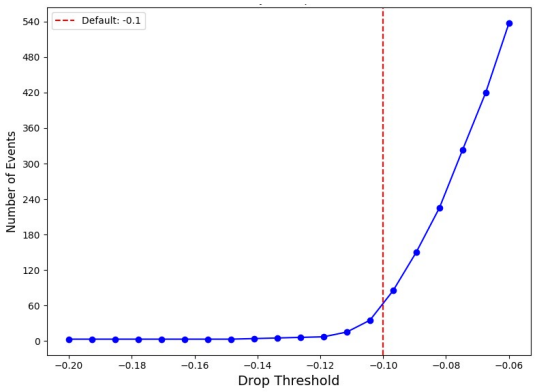

Figure C.11: Sensitivity of Condition A1., Wanssum

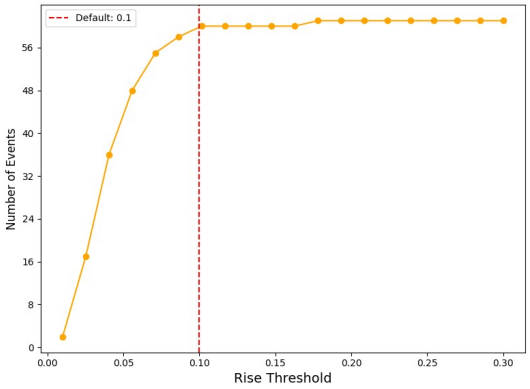

Figure C.12: Sensitivity of Condition A2., Wanssum

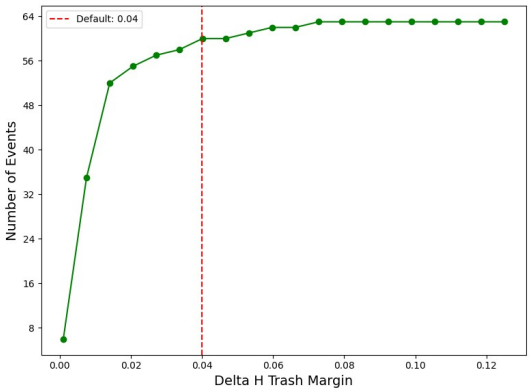

Figure C.13: Sensitivity of Condition A3., Wanssum

Figure C.14 shows a much higher number of events at lower values compared to the other sites, and the decline is more abrupt as values increase. This suggests that sharp drop events are more concentrated in smaller values for Conditon B1. at Wanssum, making it more sensitive to lower values. The chosen condition of 0.14 m balances event detection while avoiding excessive noise. The mean head loss value of 0.037 m as Conditon B2. is not significantly influenced by the selection of higher values, only smaller. Therefore, capturing meaningful events as can be seen in Figure C.15. Note that this method detects a significant amount of sharp drop events.

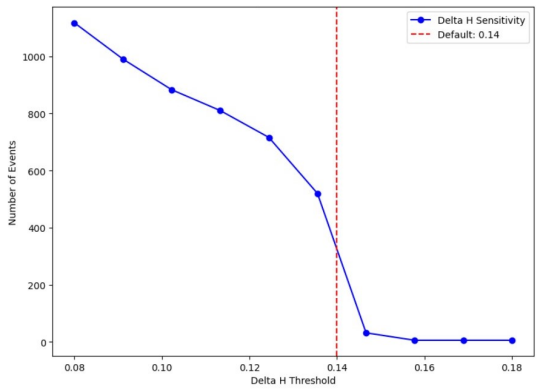

Figure C.14: Sensitivity of Conditon B1., Wanssum

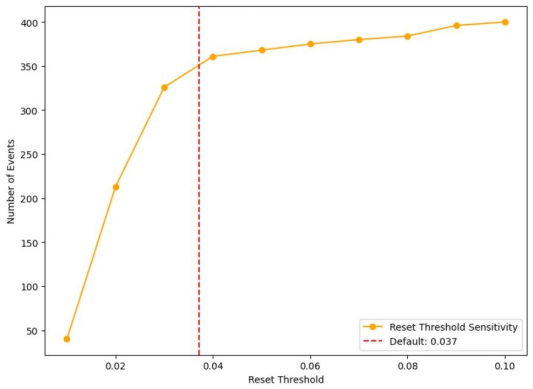

Figure C.15: Sensitivity of Condition B2., Wanssum

D

Relationship between extractions and discharge

The collected sharp drops were analyzed in relation the behavior of discharge, to detect patterns coinciding with observations made from Figure 5.6. Here it was stated that the frequency of occurrence and magnitude of the sharp drops increased with rising discharge. The first phenomenon, the increased frequency, is evident in Figure 5.7, while the increasing magnitude appears more prominent in recent years. In addition, a peak in already rising discharge can be seen in some cases. Below the water level differences up- and downstream are plotted over time alongside the discharge course for events throughout the years 2022 and 2023.

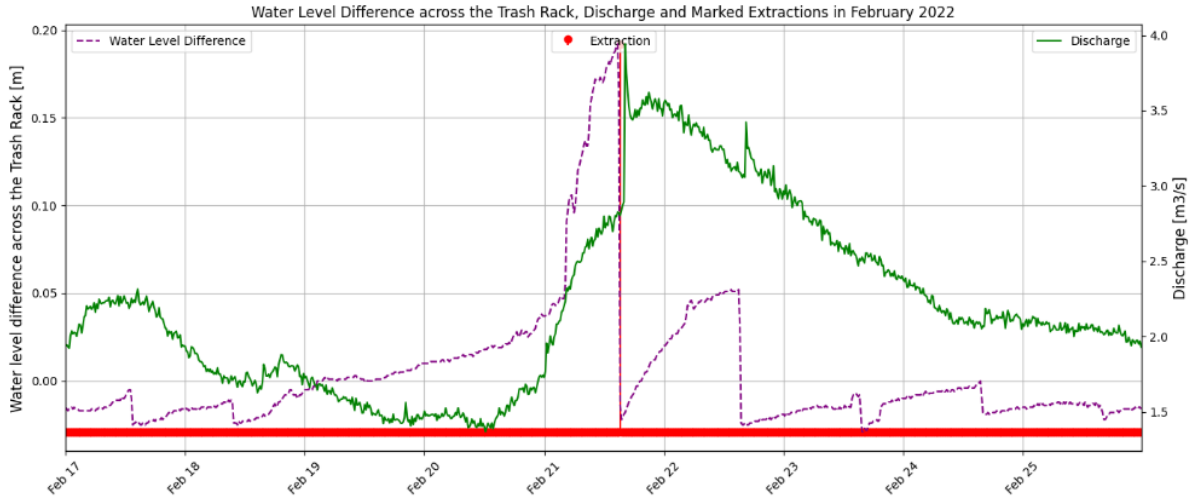

Figure D.1: Water level difference across the trash rack alongside the discharge course in February 2022

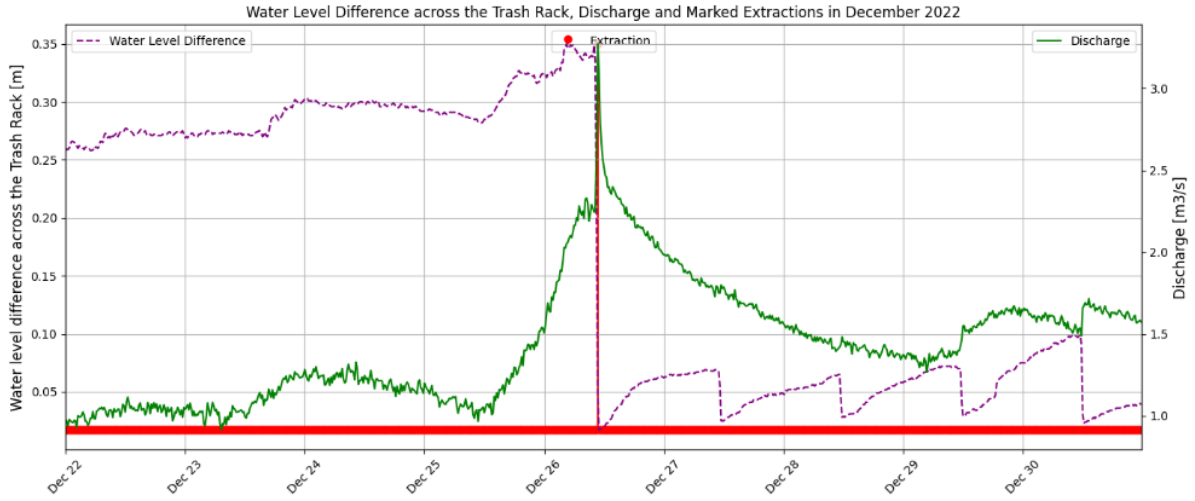

Figure D.2: Water level difference across the trash rack alongside the discharge course in December 2022

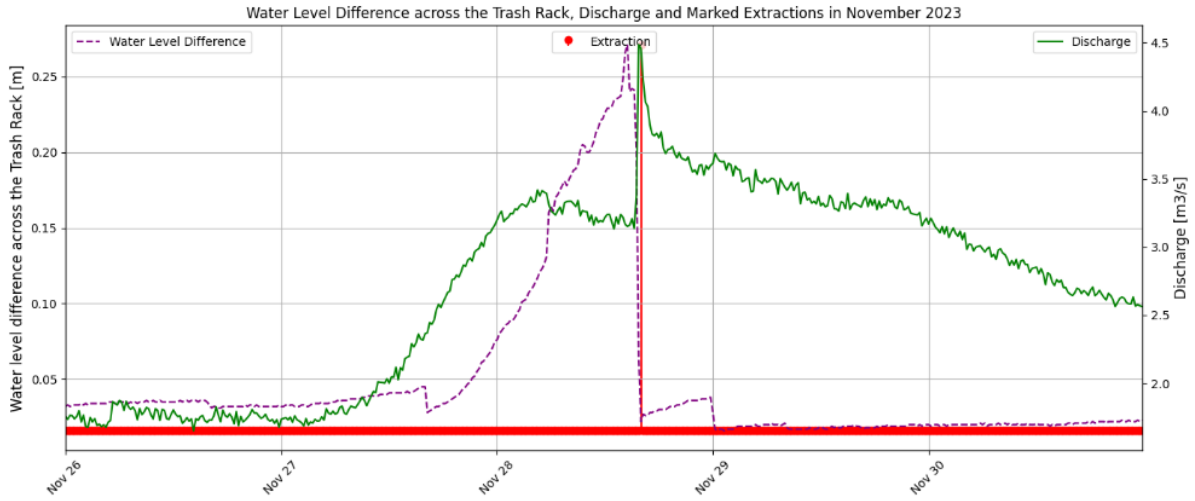

Figure D.3: Water level difference across the trash rack alongside the discharge course in November 2023